Assessing the impact of disease incidence and immunization on the resilience of complex networks during epidemics

M.D. Shahidul Islam [a], Mohammad Sharif Ullah [b], K.M. Ariful Kabir [c], *

[a] Department of Computer Science and Engineering, Green University of Bangladesh, Dhaka, Bangladesh
[b] Department of Mathematics, Feni University, Feni, Bangladesh
[c] Department of Mathematics, Bangladesh University of Engineering and Technology, Dhaka, Bangladesh

ARTICLE INFO

ABSTRACT

Disease severity through an immunized population ensconced on a physical network topology is a key technique for preventing epidemic spreading. Its influence can be quantified by adjusting the common (basic) methodology for analyzing the percolation and connectivity of contact networks. Stochastic spreading properties are difficult to express, and physical networks significantly influence them. Visualizing physical networks is crucial for studying and intervening in disease transmission. The multi-agent simulation method is useful for measuring randomness, and this study explores stochastic characteristics of epidemic transmission in various homogeneous and heterogeneous networks. This work thoroughly explores stochastic characteristics of epidemic propagation in homogeneous and heterogeneous networks through extensive theoretical analysis (positivity and boundedness of solutions, disease-free equilibrium point, basic reproduction number, endemic equilibrium point, stability analysis) and multi-agent simulation approach using the Gilespie algorithm. Results show that Ring and Lattice networks have small stochastic variations in the ultimate epidemic size, while BA-SF networks have disease transmission starting before the threshold value. The theoretical and deterministic aftermaths strongly agree with multi-agent simulations (MAS) and could shed light on various multi-dynamic spreading process applications. The study also proposes a novel concept of void nodes, Empty nodes and disease severity, which reduces the incidence of contagious diseases through immunization and topologies.

1. Introduction

Humans from diverse societies or communities are connected through networks in real-world phenomena as the world comprises human social interactions. In social networks, nodes symbolize individuals, while edges characterize the connection between two individuals. As networks are not uniform in structure, spreading infection on networks is also distinct in diverse communities. If any disease spreads in physical networks (human-human interaction), disease transmission dynamics show different physical appearances, heterogeneous infection rates, levels of intimacy, and contact

frequency for realistic diseases. People's immunity levels for combating infectious diseases vary due to physical and social conditions, naturally achieving immunity, innate immunity, vaccination, and hygienic food habits (Kabir & Ullah, 2023; Ullah et al., 2022a, 2022b). The present research focuses on how an individual's immunity influences disease transmission on diverse homogeneous and heterogeneous networks, which can assist in providing policymakers with more qualitative and quantitative insights to stop an epidemic. To understand the disease dynamics more rigorously, we initially consider ER-random (Erdős & Rényi, 1959), Random regular (Bollobás, 2001), BA scale-free (SF) (Barabási & Albert, 1999), Ring (Watts & Strogatz, 1998a), Lattice (Newman et al., 2006), and the small world (WS) (Watts & Strogatz, 1998b) network topologies to investigate the impact of disease incidence in dynamic networks. Then, to stop the transmission of newly developing or reemerging infectious illnesses, we added void nodes of the perfect immunized individual to the aforementioned social network. Employing such immunized individuals, nonetheless, incurs infections in every individual in society.

J. A. Barnes (Barnes, 1954) is credited with introducing the concept of social networks in 1954 through an anthropology paper focused on the social aspects of connections between hubs within a network. In 1985, Klovdahl (Klovdahl, 1985) utilized social network analysis (**SNA**) for the first time in epidemiological models. Additionally, the network structure is vital in developing effective interventions or awareness initiatives (Christakis & Fowler, 2010), which gives practical tools for understanding the "dynamic disease's" underlying environment and tracking the development and effect of different strategies. The identification of groups of persons, peripheral individuals, and the explanation of the network's macrostructure in a manner that should influence disease transmission rate as individuals are interconnected, which impacts social networks. In contrast, the person (node) with the most connections (edges) is more likely to come into contact with other people and, consequently, is more susceptible to infection. Thus, the complex social networks provide a realistic technique for analyzing the spread of epidemics compared to the limitations of ODE compartmental models (Atifa et al., 2022; Haq et al., 2023; Kabir et al., 2020; Kabir and Tanimoto, 2019a, 2019b; Ngonghala et al., 2023).

Contemporary research has shown that the topology of social, biological, and technological networks in the real world has many epidemiological properties that govern how diseases emerge in various networks and how individuals behave regarding the disease transmission process directly related to public health. Numerous researchers have examined the transmission of epidemic diseases in physical networks, namely, BA scale-free and small-world (WS) networks (Moreno et al., 2002; Wang et al., 2016; Zhang & Fu, 2009; Zhang & Jin, 2011; Zhang & Sun, 2014). Following analyzing many epidemic models on networks (Goltsev et al., 2012; Yuan et al., 2013a, 2013b), Zhu and Wang (Zhu & Wang, 2017) studied a modified SIR model to examine the transmission of rumors across BA and WS complex social networks. For example, scale-free networks can withstand arbitrarily but are highly susceptible to purposeful assaults from densely interconnected nodes (Boguna et al., 2003; Callaway et al., 2000). SF networks, which follow power-law distributions, describe the number of heterosexual partners reported by diverse populations (Boguna et al., 2003; Callaway et al., 2000; Liljeros et al., 2001). Pastor-Satorras and Vespignani established the existence of an epidemic threshold in finite SF networks in their investigation of the SIS model (Liljeros et al., 2001; Newman, 2003; Pastor-Satorras and Vespignani, 2001, 2002a, 2002b). Yuan et al. (Yuan et al., 2018) introduced a SIR model with two susceptible groups and investigated it on complex networks, where human interactions are seen as an SF social network. Chen et al. (Chen et al., 2018) present an SIS-type disease transmission model including age-dependent infection, birth, and death on a heterogeneous network to evaluate epidemic disease propagation and dynamic behavior. Wei (Wei, 2024) researched a network-based SIR epidemic model incorporating a saturated treatment function. In addition, many epidemic diseases emerge in regions where a scale-free network is predicted to exist, such as in locations where human interactions occur. Tatsukawa et al. (Tatsukawa et al., 2022) thoroughly investigate the stochastic outcomes by modifying the topology, average degree, and starting number of infected individuals in agent-based simulations for networked SIR processes. Li and Yousef provide in (Li & Yousef, 2019) the network-based SIR epidemic model that includes a treatment function that has reached its maximum potential. In their study, Lou and Ruggeri (Lou & Ruggeri, 2010) investigate the epidemic threshold and transmission dynamics of sexually transmitted diseases (STDs) by using multiple susceptible-infected-removed-susceptible models on scale-free networks. Wang et al. (Wang et al., 2017) present a knowledge transmission model and create mean-field equations that characterize the knowledge transmission process's dynamics by considering the self-learning mechanism in a complex network. These equations describe how information is passed from one person to another. According to Kuga and Tanimoto, introducing void nodes into a network creates a more diverse network and minimizes the final epidemic size (Kuga & Tanimoto, 2022).

Our initial model included birth and death rates to explore theoretical and numerical aspects. In subsequent simulations, we maintained a constant population within the network by assuming equivalent birth and death rates. Furthermore, we integrated the concept of birth and death agents into our epidemic model by examining the function of the Empty node, which involved the birth of agents from an empty node, contributing as susceptible agents, and the death of agents, leaving the Empty node vacant.

Based on the discussed background, the present study first explored to depict the SIR process with a multi-agent simulation (MAS) technique by borrowing the social network concepts, i.e., random (ER), random regular (RR), BA-SF, Ring, Lattice, and small world (WS) network. Due to the implementation of immunized individuals in the social network's static form into the epidemic transmission process, we propose a novel concept of void nodes, which embeds the phenomena toward immunization on the premise that including void nodes reduces the contagious disease severity. To perform multi-agent simulation, we used the Gilespie algorithm (Allen, 2008; Gillespie, 1977; Meyer & Shackelton, 2019) to model epidemics and other infectious diseases, as it allows for the inclusion of stochastic effects and individual-level heterogeneity.

1.1. Network-based SVIR epidemic model

We suggest a multiagent-based epidemic SIR dynamics on a complex social network. The model presented in this research work is a mean-field approximation approach since the complex network is dynamic, and the linkages are constantly rewired throughout the dynamics of an epidemic. The analyzed network is allocated for N, where it is either vacant or employed by a single agent, and each site in N may connect one of the states of S, I, and R.

Additionally, n groups are created for each state based on the degree of the site. For $k = 1, 2, 3, ..., n$, the maximum degree number n symbolizes the fate of those with a degree k who are susceptible (S_k), infected (I_k), and recovered (R_k). The pace at which each site's status may change varies. A healthy person from a vulnerable group may be born at a rate Λ in an empty location. If there are sick people around, a healthy member of a susceptible group gets infected by contact at a rate of β. A specific rate of recovery γ is possible for the sick person. Node mortality is equal to μ. Therefore, one can write the mean-field equations (Chen et al., 2018; Wei, 2024; Yuan et al., 2018):

$$\dot{S}_k(t) = \Lambda - \beta k S_k(t)\Theta(t) - \mu S_k(t), \tag{1.1}$$

$$\dot{I}_k = \beta k S_k(t)\Theta(t) - (\gamma + \mu)I_k(t), \tag{1.2}$$

$$\dot{R}_k = \gamma I_k(t) - \mu R_k(t). \tag{1.3}$$

If a link connects to a site of degree k, the probability that it does so is proportional to the degree of distribution $kP(k)$ (Haq et al., 2023; Kabir et al., 2020) for uncorrelated complex degree networks, then $\Theta(t)$ is represented as

$$\Theta(t) = \frac{1}{<k>} \sum_{k=1}^{n} kP(k)I_k(t), \tag{2}$$

where $P(k) > 0$, the degree distribution of the network, which satisfies the normalized equality $\sum_{k=1}^{n} P(k) = 1$, and $<k> = \sum_{k=1}^{n} kP(k)$ symbolizes the average degree of the network.

The proposed model (1.1−1.3) with equation (2) and the initial condition $S_k(0) = S_k^0, I_k(0) = I_k^0, R_k(0) = R_k^0$ must be satisfied with inequality $0 < S_k^0 + I_k^0 + R_k^0 \leq 1$, which describes the dynamics of the basic SIR model on uncorrelated networks with degree distribution $kP(k)$. Any system (1.1−1.3) solution starting from the nonnegative cone R_+^{3n} is shown to stay nonnegative. Therefore, we examine the R_+^{3n} model (1.1−1.3) in the following sections. Additionally, combining the four equations in the model (1.1−1.3) results in

$$\frac{d}{dt}(S_k + I_k + R_k) = \Lambda - \mu(S_k + I_k + R_k) \tag{3.1}$$

Therefore, $\limsup\limits_{t \to \infty} [S_k(t) + I_k(t) + R_k(t)] \leq \frac{\Lambda}{\mu}$. As a result, the feasible compact region

$$\Pi = \left\{ S_1, I_1, R_1, ..., S_k, I_k, R_k \right\} \in R_+^{3n} : S_k(t) + I_k(t) + R_k(t) \leq \frac{\Lambda}{\mu}, \tag{3.2}$$

contains a positive invariant concerning the model (1.1−1.3) that is included in the nonnegative cone of R_+^{3n} with $1 \leq k \leq n$.

1.2. Networks

Euler's solution to a bridge problem in 1735 started graph theory, developing network science (Euler, 1741; Alexanderson, 2006). Moreno extended the concept of networks to social systems, leading to the study of social networks (Moreno, 1934). Network science has applications in many fields, including statistical physics, computer science, biology, economics, finance, and public health (Barabási, 2016; Caldarelli & Catanzaro, 2012; Cayley, 1857; Hamilton, 1858; Kirchhoff, 1845; Newman, 2018). In a physical network, a node represents an individual, while edges represent their connections or relationships. The degree of a node in a social network refers to the number of neighbors. A hub in a social network is a node with a significantly higher number of links than others, indicating its importance or influence within the network. With the assumption of epidemic dynamics (equation (1.1)-(1.3)) by the set of the system of ordinary differential equations, we consider six distinct social networks: Erdös and Rényi (ER) random, Random Regular (RR), Barabasi and Albert (BA) scale-free, Ring, Lattice and WS (Watts and Strogatz) small-world network.

Different network structures have been applied to epidemic spread modeling. In an Erdös-Rényi random network, connections between individuals are formed randomly, resulting in a Poisson degrees distribution. On the other hand, random regular (RR) networks have a uniform degree distribution, where each individual in the society has the same number of connections. In Barabasi-Albert scale-free networks, the degree distribution is uneven, following a power law, where a few individuals have many connections, and many individuals have few connections, which can significantly impact epidemic spread. A ring network, where each node is connected to its two neighbors in a cycle, is a simple structure used to model the

spread of an epidemic. Lattice graphs are suitable for modeling epidemics in populations with a well-defined local structure, such as a two-dimensional grid. The small-world network, built on a regular lattice where each node is connected to its nearest neighbors, replicates the spread of diseases in populations where people have close and distant interactions.

1.3. Erdös and Rényi (ER) random network

Erdös and Rényi's (ER) work on random graphs, where vertices are randomly connected, significantly contributed to establishing network science (Erdös & Rényi, 1960; Erdős & Rényi, 1959). The random graph model, despite its differences from existing networks, is crucial for showing the existence of graphs meeting particular criteria or for explaining almost universal attributes. The easiest method for constructing a random graph is to draw connections between possible pairs of vertices with probability p until all pairs have been connected. The equation for the number of edges in an ER graph with N nodes and probability p is:

$$E = N(N-1)\frac{p}{2} \tag{4.1}$$

where N is the total number of nodes in the graph and $p = \frac{<k>}{N-1}$ is the probability that an edge will connect any two nodes. This equation holds because there are $\frac{N(N-1)}{2}$ possible pairs of nodes in the graph and each pair of nodes is connected by an edge with a probability p.

1.4. Random regular (RR) network

In 1979, mathematician Joel Spencer suggested the idea of a random regular graph, where each vertex has the same degree, and edges are given arbitrarily subject to this constraint (Bollobás, 2001). Random regular graphs have intriguing characteristics, such as a small diameter and a considerable girth, and are still a hot topic for study in computer science, mathematics, and related disciplines today. They provide insights into the structure and behavior of systems like social networks, transportation networks, biological networks, and information science. The equation for the number of edges in an RR graph with N nodes and average degree $<k>$ is:

$$E = <k>\frac{N}{2} \tag{4.2}$$

1.5. Barabasi and Albert (BA) scale-free network

Barabasi and Albert proposed a mathematical model of network evolution with hubs and a scale-free degree distribution (Barabási & Albert, 1999). New nodes are added to an initial nucleus and preferentially attached to existing nodes with numerous connections. This model accounts for the properties of many existing networks, like social media, biology, physics, and computer science. The equation for the number of edges in a BA network with N nodes is:

$$E = m(N-1) \tag{4.3}$$

where m is the number of edges added to the graph at every time during the initial growth phase of the network.

$$<k> = 2m.$$

1.6. Ring network

The ring graph is a simple structure studied by mathematicians and computer scientists for many years, where each node is linked to its two neighbors in a cycle of nodes (Watts & Strogatz, 1998a). It is still a topic of study today and is used as a model for various systems, including social networks, transportation networks, and power grids. Ring graphs are also used to simulate distributed algorithms and communication networks. The formula for determining the number of edges in a ring network with N nodes is:

$$E = \frac{<k>N}{2} \tag{4.4}$$

1.7. Lattice

Lattice (Newman et al., 2006) graphs have a stable, grid-like structure that mathematicians and physicists have studied for decades. They have applications in various fields, including statistical physics, materials research, and computer science. Lattice graphs are used to model the structure and complexity of algorithms, optimization problems, and the dynamics of social and communication networks. The number of edges in a two-dimensional square lattice graph can be computed for N nodes and $<k>$ average degrees using the following formula:

$$E = <k> \frac{N}{2} \tag{4.5}$$

1.8. Watts and Strogatz (WS) small-world network

Milgram and Travers (Milgram, 1967; Travers & Milgram, 1969) conducted tests in 1967 and found that human social networks have short path lengths, leading to "six degrees of separation." Watts and Strogatz (Watts & Strogatz, 1998b) attempted to create small-world networks in 1998 by starting with a regular ring lattice and adding randomness. Small-world networks have diverse architectures and connection patterns, resulting in a variable equation for the relationship between the number of nodes and edges. For a small-world network with N nodes and average degree $<k>$, the number of edges can be estimated by,

$$E = <k> \frac{N}{2}$$

where E is the total number of edges in the network. This equation assumes that the network is sufficiently large and well-connected and that the degree distribution is approximately Poisson or exponential. In a small-world network, the average degree $<k>$ can be tuned by adjusting the rewiring probability, which controls the balance between regularity and randomness in the network structure. The above equation approximates and may not hold strictly for all small-world networks, especially those with highly skewed degree distributions or other non-random features.

1.9. Theoretical analysis

Positivity and boundedness of solutions.

Lemma 1. *Let us assume that the solution $(S_1, I_1, R_1, \ldots S_n, I_n, R_n)$ of the proposed system illustrated in* equation (1.1)-(1.3) *for the given initial condition , where $\Theta(0) > 0$. Therefore, $0 < S_k(t) < 1, 0 < I_k(t) < 1, 0 < R_k(t) < 1,$ and $\Theta(t) > 0, \forall\ t > 0$, where $k = 1, 2, 3, \ldots, n$.*

Proof: Firstly, consider that $\Theta(t) > 0, \forall\ t > 0$. Then one can write from equation (2)

$$\dot{\Theta}(t) = \frac{1}{<k>} \sum_{k=1}^{n} kP(k)\dot{I}_k(t)$$

$$= \frac{1}{<k>} \sum_{k=1}^{n} kP(k)(\beta k S_k(t)\varphi(t) - (\gamma + \mu)I_k(t))$$

$$= \Theta(t)\left(\frac{1}{<k>} \sum_{k=1}^{n} \beta k^2 P(k) S_k(t) - (\gamma + \mu) \right).$$

Then we can write,

$$\Theta(t) = \Theta(0)exp\left\{ -(\gamma + \mu)t + \int_0^t \frac{\beta k^2 P(k)}{<k>} \sum_{k=1}^{n} S_k(v)dv \right\}.$$

As $\Theta(0) > 0$, and $\Theta(t) > 0, \forall\ t > 0$.

According to the initial condition, $S_k(0) \geq 0, V_k(0) \geq 0$. Then from the continuity of susceptible individuals $S_k(t), \exists\ \delta > 0$, which implies that $S_k(0) > 0$ for $t \in (0, \delta)$. Therefore, we have to show that $S_k(t) > 0\ \forall\ t$. Otherwise, we can locate $t_0 \geq \delta > 0$ such that $S_k(t_0) = 0$ and $S_k(t) > 0$ for some $t \in (0, t_0)$. Thus, from equation (1.1), we have,

$$\dot{S}_k(t) = \Lambda > 0.$$

It means the fact that $S_k(t_0) < 0$ for some $t \in (0, t_0)$ seems to be in a contradiction. As a result, $S_k(t) > 0 \ \forall \ t$. The following relationship can be derived from equation (1.2) using the positivity of $S_k(t)$ and $\Theta(t)$:

$$\dot{I}_k - \beta k S_k(t)\Theta(t) + (\gamma + \mu)I_k(t) > 0 \ for \ t > 0.$$

Then, we can write,
$I_k(t) > I_k(0)\exp(-\gamma - \mu)t \geq 0$ for the positivity of $S_k(t)$ and $\Theta(t)$.
Therefore, $I_k(t) > 0 \ \forall \ t$.
And finally, we can show that $R_k(t) > 0 \ \forall \ t$.
Here, the total population, $N_k(t) = S_k(t) + I_k(t) + R_k(t)$, where $k = 1, 2, 3, ..., n$.
Then, $\dot{N}_k(t) = \dot{S}_k(t) + \dot{I}_k(t) + \dot{R}_k(t)$.
Substituting the value of $\dot{S}_k(t), \dot{I}_k(t), \dot{R}_k(t)$ from equation (1.1)-(1.3) in the above equation, we have (when $\Lambda = \mu$ i.e., the population is static).
$\dot{N}_k(t) = 0 \ \forall \ t \geq 0$, which assures that the sum of the population $N_k(t)$ is fixed.
Now, $N_k(t) = S_k(t) + I_k(t) + R_k(t) = 1 \ \forall \ t > 0$. As $S_k(t) > 0, I_k(t) > 0$ and $R_k(t) > 0$; as a result, we accomplish that $0 < S_k(t) < 1, 0 < I_k(t) < 1, 0 < R_k(t) < 1, and \ \Theta(t) > 0, \forall \ t > 0$, which concludes the proof.

1.10. Disease-free equilibrium point

The equilibrium at which the population is free of infection, i.e., all affected classes will have a value of zero, is known as the "disease-free equilibrium," and the symbol represents it $\boldsymbol{E}_0 = (E_0, ..., E_0)^T \in \boldsymbol{F}^n$. Thus, $E_0 = (1, 0, 0, 0, ..., 1, 0, 0, 0)$ and $\boldsymbol{F} = \mathbb{R}^4$.

1.11. Basic reproduction number R_0 and endemic equilibrium point (EEP) E_*

The basic reproduction number R_0, a threshold value of an average number of secondary case counts a typical infected person produces throughout their whole infectious period in a fully susceptible community. It determines the global dynamics of epidemic systems and is also a significant indicator of the control efforts for infectious diseases (Diekmann et al., 1990; Driessche & Watmough, 2002). For epidemic models in homogeneous/heterogeneous populations, Diekmann et al. (Diekmann et al., 1990) provided a precise mathematical description and calculation of the basic reproduction number in 1990. Van den Driessche and Watmough (Driessche & Watmough, 2002) simplified this formulation, which applies to most ODE compartmental disease models. Generally speaking, the global dynamics of epidemic models are governed by the disease threshold $R_0 = 1$. In particular, if $R_0 < 1$, the endemic equilibrium is locally asymptotically stable; conversely, if $R_0 > 1$, the disease-free equilibrium is locally asymptotically unstable. In the following section, we now demonstrate the existence of a threshold value R_0 that is connected to equation (1.1)-(1.3) parameters and the network topology such that if $R_0 > 1$, an endemic equilibrium occurs.

Lemma 2. *Let us define the threshold value*

$$R_0 = \frac{\beta <k^2>}{(\gamma + \mu) <k>},$$

where $<k^2> = \sum_{k=1}^{n} k^2 P(k)$. Thus, the system of nonlinear equation (1.1)-(1.3) has an endemic equilibrium point denoted by E_* whenever $R_0 > 1$.

Proof: To determine the EEP of the heterogeneous-based network model, we suppose $E_* = (S_1^*, I_1^*, R_1^*, ...S_n^*, I_n^*, R_n^*)$ is an EEP of the proposed model. Thus, E_* must be satisfy

$$\Lambda - \beta k S_k(t)\Theta(t) - \mu S_k(t) = 0,$$

$$\beta k S_k(t)\Theta(t) - (\gamma + \mu)I_k(t) = 0, \qquad\qquad (5.1)$$

$$\gamma I_k(t) - \mu R_k(t) = 0, k = 1, 2, 3, ..., n.$$

Then

$$S_k^* = \frac{\Lambda}{\beta k \Theta + \mu},$$

$$I_k^* = \frac{\Lambda \beta k \Theta}{(\beta k \Theta + \mu)(\gamma + \mu)},$$

$$R_k^* = \frac{\gamma}{\mu} \left[\frac{\Lambda \beta k \Theta}{(\beta k \Theta + \mu)(\gamma + \mu)} \right] \tag{5.2}$$

Replacing the value of I_k in equation (2), we get

$$\Theta \left(1 - \frac{1}{<k>} \sum_{k=1}^{n} \frac{\Lambda \beta k^2 \Theta P(k)}{(\beta k \Theta + \mu)(\gamma + \mu)} \right) = 0$$

Let,

$$F(\Theta) = 1 - \frac{1}{<k>} \sum_{k=1}^{n} \frac{\Lambda \beta k^2 \Theta P(k)}{(\beta k \Theta + \mu)(\gamma + \mu)}$$

$$\Rightarrow F(1) = 1 - \frac{1}{<k>} \sum_{k=1}^{n} \frac{\Lambda \beta k^2 P(k)}{(\beta k + \mu)(\gamma + \mu)}$$

$$> 1 - \frac{1}{<k>} \sum_{k=1}^{n} \frac{\beta k^2 P(k)}{\beta k} = 0.$$

Here, F is continuous on the close interval $[0, 1]$, and according to the Intermediate Value Theorem, if $F(0) < 0$, then there exists a positive solution $F(\Theta) = 0$, which implies that $R_0 > 1$. Therefore, we will obtain the EEP after replacing the value of the positive solution, which concludes the proof of the above lemma.

1.12. Stability analysis of the disease-free and endemic equilibrium point

This section presents the stability analysis of the DFE point $\boldsymbol{E}_0$ and EEP $\boldsymbol{E}_*$. Here, we demonstrate that $\boldsymbol{E}_0$ is locally as well as globally asymptotically stable (GAS) and attractive when $R_0 < 1$. On top of that, then represent the instability and the endemic equilibrium point $\boldsymbol{E}_*$ is asymptotically stable for $R_0 > 1$.

Theorem 1. *The DFE point $\boldsymbol{E}_0$ of the proposed vaccinated SVIR model is locally asymptotically stable (LAS) if $R_0 < 1$ and unstable when $R_0 > 1$.*

Proof: *Suppose, $S_k(t) = x_k(t), I_k(t) = y_k(t)$.*

Here, $x_k(t), y_k(t)$ and $z_k(t)$ is the small perturbation of $\boldsymbol{E}_0$. Then, we can write the linear system as follows:

$$\dot{x}_k(t) = \Lambda - \mu x_k(t) - \frac{\beta k}{<k>} \sum_{k=1}^{n} k P(k) y_k(t),$$

$$\dot{y}_k(t) = -(\gamma + \mu) y_k(t) + \frac{\beta k}{<k>} \sum_{k=1}^{n} k P(k) y_k(t),$$

$$\dot{z}_k(t) = \gamma y_k(t) - \mu z_k(t). \tag{6}$$

Then we can write,

$$\frac{d}{dt} \begin{pmatrix} x_1(t) \\ y_1(t) \\ z_1(t) \\ \vdots \\ x_n(t) \\ y_n(t) \\ z_n(t) \end{pmatrix} = P \begin{pmatrix} x_1(t) \\ y_1(t) \\ z_1(t) \\ \vdots \\ x_n(t) \\ y_n(t) \\ z_n(t) \end{pmatrix},$$

where,

$$J(\boldsymbol{E_0}) = \begin{bmatrix} -\mu & U_1q_1 & 0 & 0 & U_1q_2 & 0 & \cdots & 0 & -U_1q_n & 0 \\ 0 & -(\gamma+\mu)+U_1q_1 & 0 & 0 & -(\gamma+\mu)+U_1q_2 & 0 & \cdots & 0 & U_1q_n & 0 \\ 0 & \gamma & -\mu & 0 & 0 & 0 & \cdots & 0 & 0 & 0 \\ 0 & -U_2q_1 & 0 & -\mu & -U_2q_2 & 0 & \cdots & 0 & -U_2q_n & 0 \\ 0 & U_2q_1 & 0 & 0 & -(\gamma+\mu)+U_2q_2 & 0 & \cdots & 0 & U_2q_n & 0 \\ 0 & 0 & 0 & 0 & \gamma & -\mu & \cdots & 0 & 0 & 0 \\ \vdots & \vdots & \vdots & \vdots & \vdots & \vdots & \ddots & \vdots & \vdots & \vdots \\ 0 & -U_nq_1 & 0 & 0 & -U_nq_2 & 0 & \cdots & -\mu & -U_nq_n & 0 \\ 0 & U_nq_1 & 0 & 0 & U_nq_2 & 0 & \cdots & 0 & -(\gamma+\mu)+U_nq_n & 0 \\ 0 & 0 & 0 & 0 & 0 & 0 & \cdots & 0 & \gamma & -\mu \end{bmatrix}$$

Here,

$$U_k = \frac{\beta k}{<k>}, q_k = kP(k), \text{for } k = 1, 2, 3, \ldots, n.$$

Thus, the characteristic polynomial of Jacobian matrix $J(\boldsymbol{E_0})$ has n eigenvalues, which are equal to $-\mu, -\mu,$ and the $(n-2)th$ eigenvalue is

$$\sum_{k=1}^{n} U_kq_k - (\gamma+\mu) = (\gamma+\mu)(R_0 - 1) < 0.$$

As all eigenvalues of the Jacobian matrix $J(\boldsymbol{E_0})$ are negative if $R_0 < 1$, therefore, by the Routh-Hurwitz principle (Martcheva, 2015), $\boldsymbol{E_0}$ is LAS. Alternatively, $\boldsymbol{E_0}$ is unstable when $R_0 > 1$, because of positive eigenvalues, concludes the proof of the above theorem.

Theorem 2. *The DFE point $\boldsymbol{E_0}$ of the proposed vaccinated SIR model is globally asymptotically stable (GAS) and attractive when $R_0 \leq 1$.*

Proof: (1st part).

The Lyapunov function $L(t)$ (Yang et al., 2019; Yang & Xu, 2018) of the proposed model for $t \geq 0$ is as follows:

$$L(t) = \sum_{k=1}^{n} \frac{kP(k)}{<k>}\{[S_k(t) - 1 - \ln S_k(t)] + I_k(t)\}. \tag{7.1}$$

Then

$$\dot{L}(t) = \sum_{k=1}^{n} \frac{kP(k)}{<k>}\left\{\left(1 - \frac{1}{S_k(t)}\right)\dot{S}_k(t) + \dot{I}_k(t)\right\} \tag{7.2}$$

Substitute the value of $\dot{S}_k(t), \dot{I}_k(t)$ in equation (7.2), we get

$$\dot{L} = \sum_{k=1}^{n} \frac{kP(k)}{<k>}\left\{\left(1 - \frac{1}{S_k}\right)[\Lambda - \beta kS_k\Theta - \mu S_k] + [\beta kS_k\Theta - (\gamma+\mu)I_k]\right\},$$

$$= \sum_{k=1}^{n} \frac{kP(k)}{<k>}\left[\Lambda - \beta kS_k\Theta - \mu S_k - \frac{\Lambda}{S_k} + \beta k\Theta + \mu + \beta kS_k\Theta - (\gamma+\mu)I_k\right]$$

$$= \sum_{k=1}^{n} \frac{kP(k)}{<k>}\left[\Lambda - \mu S_k - \frac{\Lambda}{S_k} + \beta k\Theta + \mu - (\gamma+\mu)I_k\right]$$

$$= \sum_{k=1}^{n} \frac{kP(k)}{<k>}\Lambda\left[1 - \frac{\mu S_k}{\Lambda} - \frac{1}{S_k} + \frac{\mu}{\Lambda}\right] + \sum_{k=1}^{n} \frac{kP(k)}{<k>}[\beta k\Theta - (\gamma+\mu)I_k].$$

As $\Lambda = \mu$ and $0 < S_k(t) < 1,$ then the first and the second term of $\dot{L}(t)$ is negative. Thus,

$$\dot{L}(t) < \sum_{k=1}^{n} \frac{kP(k)}{<k>}[\beta k\Theta - (\gamma + \mu)I_k(t)]$$

$$= \beta \frac{k^2}{<k>}\Theta - (\gamma + \mu)\Theta(\text{t}).$$

Since $0 < I_k(t) < 1$ for $k = 1, 2, 3, ..., n$ and the probability of taken edge, which is linked to an infected individual $0 < \Theta(\text{t}) < 1$, then can write

$$\dot{L}(t) < \left[\beta \frac{k^2}{<k>} - (\gamma + \mu)\right]\Theta(t) = (\gamma + \mu)[R_0 - 1]\Theta(t) \tag{7.3}$$

It is evident that if $R_0 < 1$ then $\dot{L}(t) < 0 \ \forall \ (S_k(t), I_k(t)) \neq (1, 0)$, which follows that according to Lyapunov's theorem, the DFE point is GAS.

(2nd part).

To prove the DFE point is globally attractive when $R_0 \leq 1$, from the 1st part (equation (7.3)), we can write

$$\dot{\Theta}(t) = (\gamma + \mu)(R_0 - 1)\Theta(t).$$

Assume, $\Theta(0) = g(0)$. Then

$$\dot{g}(t) = (\gamma + \mu)(R_0 - 1)g(t).$$

Talking integration on both sides, we get

$$g(t) = g(0)e^{(\gamma + \mu)(R_0 - 1)t}. \tag{7.4}$$

Here, we have $g(t) \to 0$ when $t \to 0$, as $R_0 \leq 1$.

Using the concept of the functional differential equation's comparison theorem, we can write

$$0 \leq \Theta(t) \leq g(t), \forall \ t > 0.$$

Finally, $g(t) \to 0$ when $t \to 0$ indicates that for $= 1, 2, 3, ..., n$ $I_k(t) \to 0$. Thus, the DFE point is globally attractive for $R_0 \leq 1$.

Theorem 3. *The EEP E_* of the proposed model is unique, and GAS if $R_0 > 1$.*

Proof: The Lyapunov function L_k of the proposed model for $t \geq 0$ is as follows:

$$L_k = (S_k - S_k^* \ln S_k) + (I_k - I_k^* \ln I_k).$$

After employing the equilibrium equation and differentiating L_k, we get

$$\dot{L}_k = \left(1 - \frac{S_k^*}{S_k}\right)\left[\Lambda - \beta kS_k\Theta - \mu S_k - \Lambda + \beta kS_k^*\Theta^* + \mu S_k^*\right] + \left(1 - \frac{I_k^*}{I_k}\right)[\beta kS_k\Theta - (\gamma + \mu)I_k].$$

$$= \mu S_k^*\left(2 - \frac{S_k^*}{S_k} - \frac{S_k}{S_k^*}\right) + \left(1 - \frac{S_k^*}{S_k}\right)(\beta kS_k^*\Theta^* - \beta kS_k\Theta) + \left(1 - \frac{I_k^*}{I_k}\right)\left[\beta kS_k\Theta - \frac{I_k}{I_k^*}\beta kS_k^*\Theta^*\right]$$

$$\leq \left(1 - \frac{S_k^*}{S_k}\right)(\beta kS_k^*\Theta^* - \beta kS_k\Theta) + \left(1 - \frac{I_k^*}{I_k}\right)\left(\beta kS_k\Theta - \frac{I_k}{I_k^*}\beta kS_k^*\Theta^*\right)$$

$$= \sum_{J=1}^{n} \frac{\beta kjP(k)}{<k>}S_k^*I_j^*\left(2 - \frac{S_k^*}{S_k} - \frac{I_jS_kI_k^*}{I_kS_k^*I_j^*} + \frac{I_j}{I_j^*} - \frac{I_k}{I_k^*}\right) \tag{7.5}$$

As

$$\frac{S_k^*}{S_k} + \frac{S_k}{S_k^*} \geq 2$$

equivalence is true if and only if

$$S_k^* = S_k.$$

Assume,

$$b_{kj} = \frac{kjP(k)}{<k>}\beta S_k^* I_j^*, H_j(I_j) = -\frac{I_j}{I_j^*} + ln\frac{I_j}{I_j^*}, \varphi(b) = 1 - b + lnb, F_{kj} = H(I_k) - H(I_j).$$

Therefore, for $b > 0$, $\varphi(b) \leq 0$. Furthermore, $b = 1$ assists in holding uniformity. Thus,

$$(7.5) \Rightarrow \dot{L}_k = \sum_{J=1}^{n} \frac{\beta kjP(k)}{<k>}S_k^* I_j^* \left(H(I_k) - H(I_j) + \varphi\left(\frac{S_k^*}{S_k}\right) + \varphi\left(\frac{I_j S_k I_k^*}{I_k S_k^* I_j^*}\right) \right)$$

$$\leq \sum_{J=1}^{n} \frac{kjP(k)}{<k>}\beta S_k^* I_j^* \left(H(I_k) - H(I_j) \right) = \sum_{J=1}^{n} b_{kj}F_{kj}.$$

Now, we will find the following matrix

$$b_{kj} = \begin{bmatrix} \dfrac{P(1)}{<k>}\beta S_1^* I_1^* & 2\dfrac{1P(1)}{<k>}\beta S_2^* I_1^* & \cdots & n\dfrac{1P(1)}{<k>}\beta S_n^* I_1^* \\ \dfrac{2P(1)}{<k>}\beta S_1^* I_2^* & 2\dfrac{2P(1)}{<k>}\beta S_2^* I_2^* & \cdots & n\dfrac{2P(1)}{<k>}\beta S_n^* I_2^* \\ \vdots & \vdots & \ddots & \vdots \\ \dfrac{nP(1)}{<k>}\beta S_1^* I_n^* & 2\dfrac{nP(1)}{<k>}\beta S_2^* I_n^* & \cdots & n\dfrac{nP(1)}{<k>}\beta S_n^* I_n^* \end{bmatrix} = \overline{A}.$$

Let us assume that the kth diagonal element of the matrix L is ψ_k, the Laplacian matrix of the matrix $\overline{A}$. According to lemma 2.1 (Guo et al., 2006), ψ_k is positive for $k = 1, 2, 3, ..., n$. Thus, L_{k^*}, F_{kj}, H_k and b_{kj} holds the theorem (3.1) and corollary 3.3 (Li & Shuai, 2010).

As a result, one can write,

$$L_k = \sum_{J=1}^{n} \psi_k L_{k^*},$$

a Lyapunov function for the system of equation (4) is well-defined in Theorem 3.1 of (Li & Shuai, 2010), specifically, $L_k \leq 0$, $\forall$ $(S_k, I_k) \in \Omega, k = 1, 2, 3, ..., n$. Using the same justification as in (Caldarelli & Catanzaro, 2012; Diekmann et al., 1990; Driessche & Watmough, 2002; Driessche and Watmough, 2002, 2002; Erdös & Rényi, 1960; Guo et al., 2006, 2008; Li & Shuai, 2010; Martcheva, 2015; Milgram, 1967; Newman, 2018; Ruoyan., 2010; Travers & Milgram, 1969; Yang et al., 2019; Yang & Xu, 2018), one can easily demonstrate that the most significant invariant subset in the case when $\dot{L}_k = 0$ is the singleton E_*. Thus, the proof concludes that E_* is GAS in Ω according to the LaSalles Invariance principle (LaSalle, 1977).

Our mathematical epidemic model's birth and death rates were incorporated solely for theoretical investigation. However, in our later simulations, we assumed that birth and death rates balance, keeping the total population constant within the network's framework. This method prevents any addition or removal of nodes or agents from the network, offering a stable basis for our analysis.

1.13. Simulation approach

In order to model the transmission of diseases across networks, we considered the MAS (multi-agents simulation) approach that randomly selected a subset of agents initially infected while the rest were considered susceptible. Generally speaking, each agent is programmed to behave according to rules, objectives, and decision-making strategies and can interact with other agents and the environment to achieve its goals. Using a discrete time-step approach following the Gillespie algorithm (Gillespie, 1977) $\tau = -\log(1 - u)/\lambda$, where u is the probability generated randomly, and λ is the total transmission rate of the society.

Agents are autonomous entities that can perceive their environment, make decisions, and act based on their objectives and available information. Interactions are how agents communicate with each other and the environment, such as exchanging information, performing actions, and updating their state. In epidemiology, suppose agents have a chance of becoming infected by their infected neighbor's agent, as determined by a randomly chosen agent from the network. In that case, they

change their status from susceptible to infected. At the same time, the transmission rate of all susceptible neighbors of the infected is updated. Alternatively, if an agent recovers from the disease in the current time step, the status changes from infected to recovered. Again, the recovery rate of all susceptible neighbors of the recovered agent will be updated accordingly. Averaging the outcomes of these realizations, we can estimate the infected, recovered, and final epidemic size (FES).

A practical and intriguing approach is determining whether targeted vaccination or interventions of a subset of the population can effectively halt and reverse the development of an epidemic. The network SIR model used, in this circumstance, is equivalent to bond percolation. At the same time, individual intervention can be seen as a fixed void node, which means that solving the immunization problem in the network SIR model is equivalent to solving a mixed percolation problem (Fig. 1). The concept of birth and death agents is also incorporated into the epidemic model by considering the role of the Empty node. Agents are born from an empty node and contribute as susceptible agents. Conversely, agents die and remain in the Empty node. In particular, randomly select a subset of immunized individuals, while some individuals are randomly infected, and the remaining individuals are susceptible. Since the immunized individuals cannot become vulnerable or infected, they remain void nodes throughout the simulation. By simulating the transmission of disease in such a manner, one can examine the consequences of immunization on the dynamics of infectious diseases. This study contributes to our understanding of the effect of vaccination on disease transmission and provides insights into the design of effective public health strategies.

2. Result and discussion

Network epidemic dynamics research is currently experiencing a surge in popularity, with recent discoveries highlighting the heterogeneity in the networks that have a crucial role in the transmission of infections. Our study findings offer new insights into the propagation of epidemics and their control policies. In addition to introducing immunization void nodes in complex networks as a new concept, physicists are also bringing new methodologies to the field of epidemiology.

The present research aims to investigate the disparities between the deterministic model and stochastic aspect as a form of multi-agent simulations (MAS). Also, the plots display the outcomes of various average degree distributions and initially infected agents. Figs. 2 and 3 show the graphical representations of the final epidemic size (FES) along with the basic reproduction number R_0 for all six networks: (a) ER, (b) RR, (c) BA, (d) Ring, (e) Lattice, and (f) WS. In each sub-figure, the line-colored red, blue, green, and violet represent the average degree $<k> = 8$, $<k> = 16$, $<k> = 64$, and $<k> = 4$, respectively. The line-colored black depicts a simple deterministic SIR epidemic model. The visual setup of Figs. 2 and 3 stated in this subsection is drawn and tracked by the consequent Figures A1-A6 in the Appendix. Due to stochasticity and randomness, each plot exhibits significant dispersion, and thus, we derived the average (ensembles) of the entire set.

Fig. 2 illustrates the line graphs of deterministic and six networks for randomly selected five initially infected individuals $I(0) = 5$. The FES colored with black in the deterministic aspect shows that the threshold value for the epidemic disease is precisely equal to 1, switching between disease-free and endemic equilibrium. Sub-panel (a) represents that the endemic equilibrium in the ER random network starts after the black line. Consequently, the disease curve is approaching the deterministic curve for increasing average degree values. RR network (subfigure (b)) shows almost the same characteristics but is slightly slow compared to ER random networks. However, BA-SF networks (c) represent that the endemic equilibrium's switching threshold value occurs before the deterministic curve. The BA network has highly connected hubs, which can perform as super-spreaders for the disease, implying that if a hub node becomes infected, the sickness may spread to the plethora of other nodes in the network. In the Ring and Lattice networks illustrated in sub-panel (d) and (e), the disease transmission process is much slower than the other four networks; in the Ring and Lattice network topologies, the endemic equilibrium starts when the value is approximately near to $R_0 = 2$ and $R_0 = 2.5$, respectively. The WS network (f) also demonstrates a similar tendency for disease transmission as ER and RR. Therefore, the endemic equilibrium starts after the deterministic line graph in all mentioned networks except the BA-SF network. All line graphs reveal an increasing tendency with the increase of average degree distribution. Finally, comparing Fig. 2 for $I(0) = 5$ and Fig. 3 for $I(0) = 50$ shows a similar but faster disease-spreading tendency.

To assess the immunization effect as void notes on the epidemic social networks, we display the 2D heatmap of FES in Fig. 4. The impact of average degree distribution and the network structures is considered to examine the influence of void nodes against contagious diseases. The final epidemic size corresponding to the basic reproduction number Ro and the fraction of immunized agent (FIA) is displayed in Fig. 4 for network topologies: Erdős-Rényi (ER) random (panel a*), random regular (RR) graph (panel b*), BA-SF (panel c*), Ring (panel d*), Lattice (panel f*), and small-world (panel e*) network. Here, panels (*-i), (*-ii), and (*-iii) display for varying average degree $<k> = 8$, $<k> = 16$, and $<k> = 64$ (for Lattice (*-i) $<k> = 4$ and (*-ii) $<k> = 8$).

As shown in Fig. 4 for the epidemic threshold and the FES, the fraction of void (immunized) nodes inserted into the existing physical network strongly affects the FES to reduce infection. Thus, the FIA of void nodes directly affects the FES when void nodes are randomly dispersed in the networks. When the average rate of connections (degree) between individuals increases, the threshold for an epidemic to transition from a disease-free state to an endemic state also increases, which means that a more significant proportion of the population must be infected before the epidemic becomes self-sustaining.
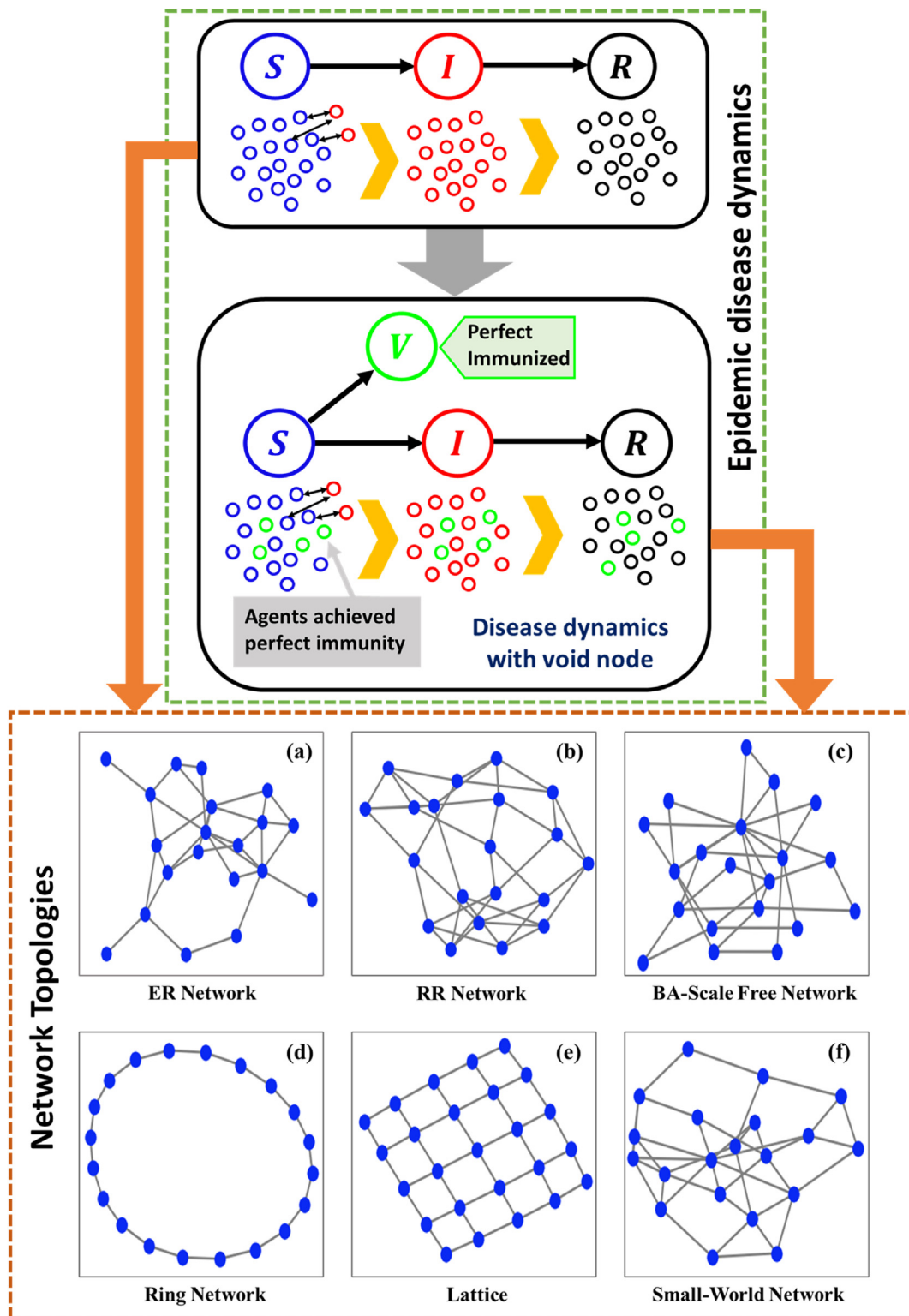
Figure: 1. A pictorial representation of epidemic disease dynamics of basic SIR (Susceptible-Infected-Recovered) model with void node and Network Topologies. Network Topological study includes Homogeneous (Random-Regular, Ring, Lattice) and Heterogeneous Networks (ER-random, BA-Scale Free, Small-World).
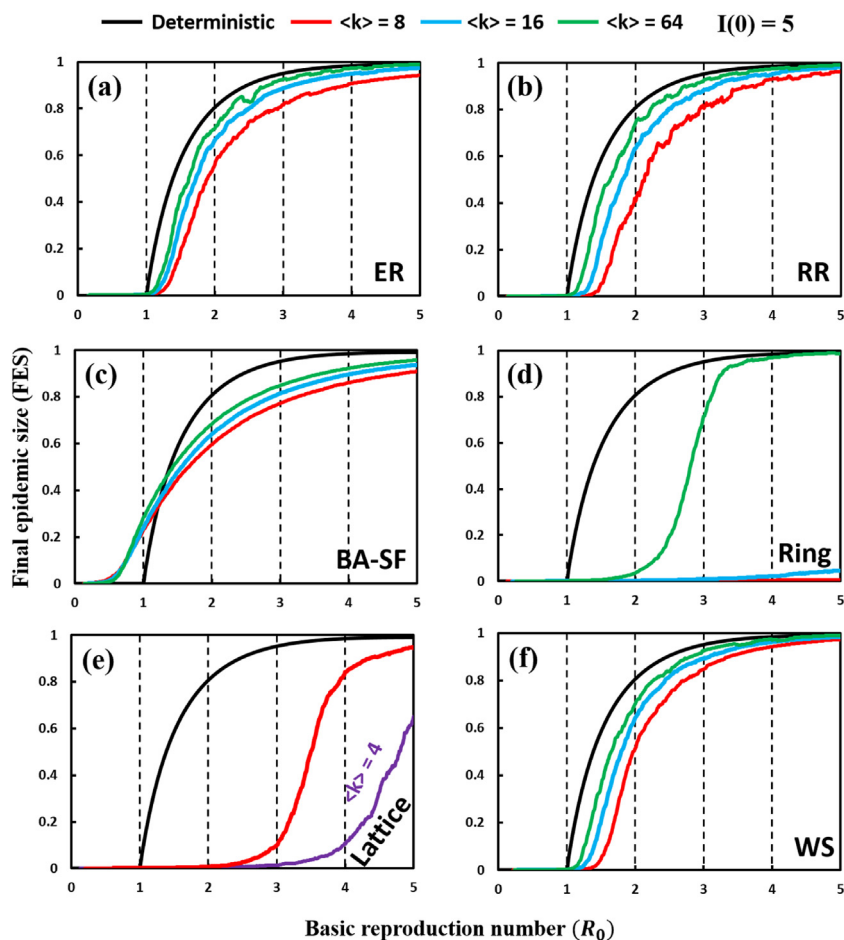
Figure: 2. Representations of the basic reproduction number (R_0) versus the final epidemic size (FES) of deterministic and **(a)** ER random, **(b)** RR, **(c)** BA-SF, **(d)** Ring, **I** Lattice, and **(f)** WS physical networks for initially infected individuals, $I(0) = 5$ with varying degrees of connectivity. The color black represents the FES of the deterministic line graph, whereas violet, green, blue, and red represent the FES of average degree $<k> = 4, 8, 16, 64$. Here, total population $N = 10^4, \gamma = \frac{1}{3}$.

The FES will also be more prominent due to the increased connections between individuals. These results are consistent with Figs. 2 and 3, as explored above. However, by introducing void nodes, the number of connections between infected agents is decreased, suppressing the transmission of the epidemic in the network because the void nodes act as barriers or buffers between infected individuals, making it more difficult for the disease to spread through the network.

All the physical networks have a basic disease-spreading tendency except scale-free networks (c-*), which occur when the endemic equilibrium begins; however, different network types have diverse tendencies regarding the transmission of infectious illnesses. Meanwhile, the average degree of all physical networks also affects disease transmission. In Fig. 4 (Panel A), we can see that the disease spreads more if the average degree increases. In an Erdos-Renyi (ER) network (a-*), connections' random and stochastic nature can create a situation where the disease spreads more easily among high-degree nodes, leading to a faster initial spread. In contrast, a Random-Regular (RR) (b-*) network exhibits a slower spread of the disease. In a BA-SF network (c-*), in the early phases of an epidemic, the existence of nodes that are heavily linked to one another, also known as hubs, might hasten the spread of the disease.

Additionally, the BA network has a power-law degree distribution, which means many nodes with low degrees and only a few with very high degrees, which can create a situation where the disease spreads rapidly among the low-degree nodes, but the epidemic takes longer to reach the high-degree hubs. As a result, endemic equilibrium occurs, but the disease can still spread rapidly in the early phases of an epidemic, particularly when highly infectious. In a ring network (d-*), the disease can continue to spread after the final epidemic size reaches its highest due to the cyclic and circular nature of the network. Therefore, the epidemic can peak relatively quickly, but the disease transmission slows considerably once most nodes become infected. In a small-world network (e−*), each node is connected to its nearest neighbors and a few randomly selected nodes,
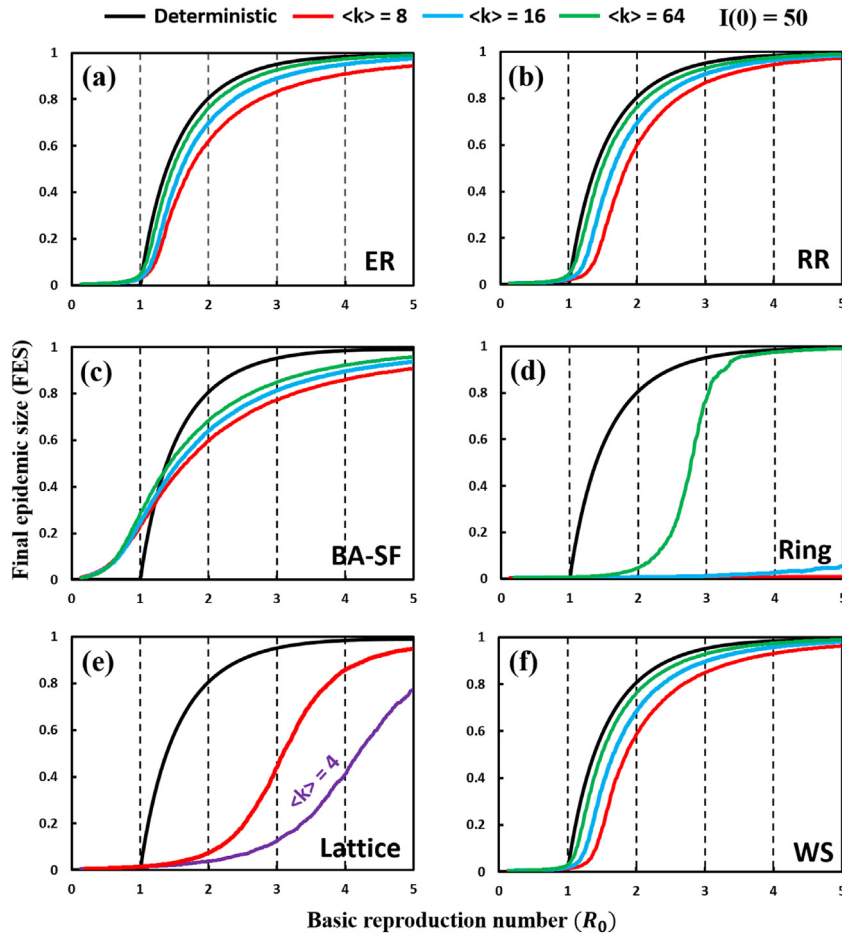
Figure: 3. Representations of the basic reproduction number (R_0) versus the final epidemic size (FES) of deterministic and **(a)** ER Random, **(b)** RR, **(c)** BA-SF, **(d)** Ring, **I** Lattice, and **(f)** WS physical networks for initially infected individuals, $I(0) = 50$ with varying degrees of connectivity. The color black represents the FES of the deterministic line graph, whereas violet, green, blue, and red represent the FES of average degree $<k> = 4, 8, 16, 64$. Here, total population $N = 10^4, \gamma = \frac{1}{3}$.

combining local clustering and long-range connections. These long-range connections can create shortcuts in the network, allowing the disease to spread more quickly between distant nodes. The presence of clustering can create a situation where the disease can spread rapidly in the early stages of the epidemic. Still, once most nodes become infected and the epidemic peaks, the disease's transmission slows considerably. However, due to the presence of shortcuts, the disease can continue to spread. Therefore, the behavior of a small-world network is distinct from other types of networks, such as a ring network, where the cyclic and circular nature of the network can slow down the transmission of the disease once the epidemic reaches its peak. In a lattice network (f-*), each node has a fixed number of neighbors connected to them in a regular pattern, resulting in a uniform distribution of degrees. As a result, the disease may spread rapidly in the epidemic's early stages. Still, disease transmission slows once the epidemic peaks and most nodes are infected because each node in the lattice network (e-*) has a limited number of neighbors, and once the disease has spread to all of them, there are no new nodes left to infect.

Fig. 4 (Panel B) presents the spreading graphs along time steps of five points taken from block f(ii) in Fig. 4 (Panel A) for the Lattice structure with degree $<k> = 8$. The points are $(R_0, FIA) = (2.0, 0.8), (3.5, 0.25), (3.5, 0.2), (4.0, 0.15)$, and $(4.5, 0.05)$, where R_0 is the basic reproduction number, and FIA is the fraction of immunized agents. The blue, red, black, and white colors display the number of susceptible, infected, recovered, and void (immunized) individuals, respectively. The leftmost panel shows the initial setup at $t = 0$. Other columns are presented for time step $t = 10, t = 30, t = 50$, and $t = 100$. The first point $(R_0, FIA) = (2.0, 0.8)$, represents that when $R_0 = 2$, and $FIA = 0.8$, the disease faded from society in just $t = 10$ days. In the current global pandemic caused by COVID-19, it has been observed that when a significant proportion of the population, around 80%, has been immunized against existing diseases, the spread of the disease is effectively stopped. This phenomenon is known as herd immunity or community immunity. However, it is essential to note that there may still be a small proportion
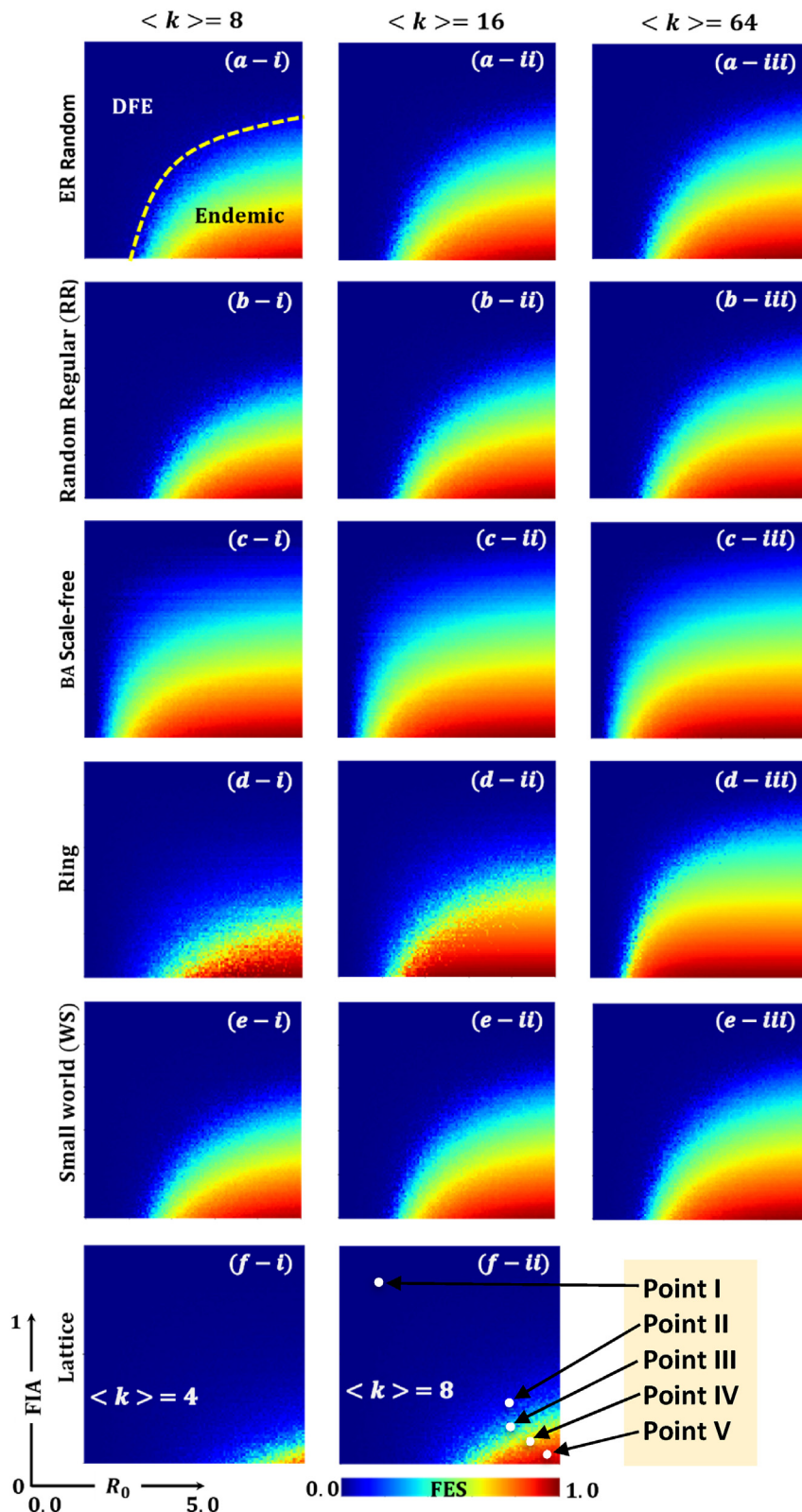
Figure: 4 (Panel A). Presented the 2D heat maps of the final epidemic size (FES) of the individuals concerning the basic reproduction number (R_0) and the fraction of immunized agents (*FIA*). Subpanels (a*), (b*), (c*), (d*), (e−*), and (f*) show for ER random, RR, BA-SF, Ring, WS, and Lattice physical networks, whereas (*-i), (*-ii), (*-iii), (*-iv), (*-v) represents the average degree $<k> = 8, 16, 64$ except for Lattice $<k> = 4, 8$. Here, total population $N = 10^4, \gamma = \frac{1}{3}$.
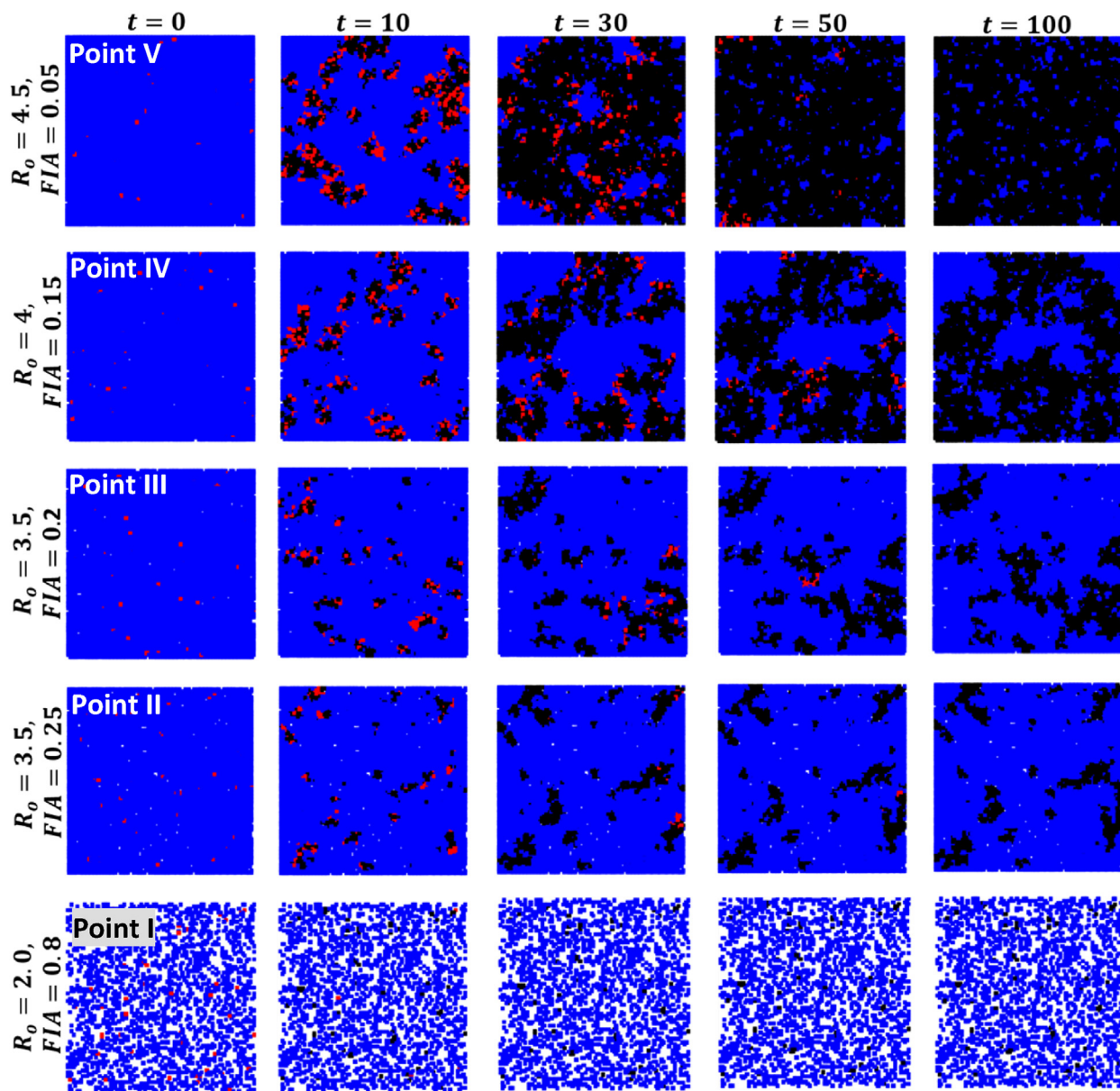
Figure: 4 (Panel B). The subsystem presents a stability analysis of five points taken from block f(ii) in Fig. 4 (Panel A) for the Lattice structure with $<k> = 8$. The points are ((R_0, FIA)= (2.0, 0.8), (3.5, 0.25), (3.5, 0.2), (4.0, 0.15), and (4.5, 0.05). The blue, red, black, and white colors display number of susceptible, infected, recovered, and void (immunized) individuals, respectively. The leftmost panel shows the initial setup at $t = 0$. Other columns are presented for time step $t = 10$, $t = 30, t = 50,$ and $t = 100$.

of individuals who are not immune despite the high FIA rate. These individuals may still be susceptible to the disease and can transmit it to others, leading to localized outbreaks or clusters of infections. The likelihood of such outbreaks occurring is influenced by several factors, including the disease's infectiousness, the vaccine's effectiveness, and the social and environmental conditions in which people live. As such, it is crucial to continue monitoring and managing the spread of infectious diseases, even in communities with high levels of immunization, to maintain the benefits of herd immunity.

The severity of a disease outbreak can be influenced by several factors related to network topology, degree distribution, and immunization. Network topology refers to the network structure or the pattern of connections between nodes. In the case of disease transmission, the network topology can influence the spread of the disease by determining how easily the infection can move from one node to another. For instance, in a network with a high degree of clustering, where nodes tend to

be more closely connected, the disease can spread quickly and easily compared to a network with low clustering. Immunization, however, can slow down or stop the spread of disease. When a certain proportion of nodes in a network are immunized, either through vaccination or prior exposure to the disease, the disease cannot spread to those nodes, which limits the number of potential new infections. Here, Figs. 5−8 illustrate the impact of the disease's severity along the basic reproduction number R_0. Moreover, the fraction of immunized agent (FIA), subtracting the deterministic outcome from six different networks, where the blue (positive) and red (negative) colors represent the less and highly severe situations. In contrast, the white color illustrates neutral situations, meaning that the network did not have a significant impact; we can consider any network.

In Fig. 5, panels A, B, and C represent the disease severity graphs for ER, RR, and WS, respectively, in which sub-panels (i), (ii), and (iii) display average degree distribution, $<k> = 8, <k> = 16,$ and $<k> = 64$, respectively. As a general tendency, we could observe that ER, RR, and WS present almost similar tendencies when the average degree distribution increases from $<k> = 8$ to $<k> = 64$. The disease is not highly severe in any community when the average degree is $<k> = 8$. However, in the case of $<k> = 64$, subfigure (iii), the blue region faded out, and the red region revealed up, illustrating a realistic scenario when the agents' number of connections is higher. Consequently, the probability of disease transmission increased and tended to a well-mixed situation that the deterministic model performed.

In the context of disease severity, the Barabasi-Albert (BA) network has been shown to have some unique features compared to other types of networks (Fig. 6). One key characteristic of the BA network is the presence of highly connected hubs, which can act as super-spreaders for the disease (independent of $<k>$) means that if a hub node becomes infected, it can spread the disease to another node in the network. More preciously, a few nodes have a very high degree, whereas few
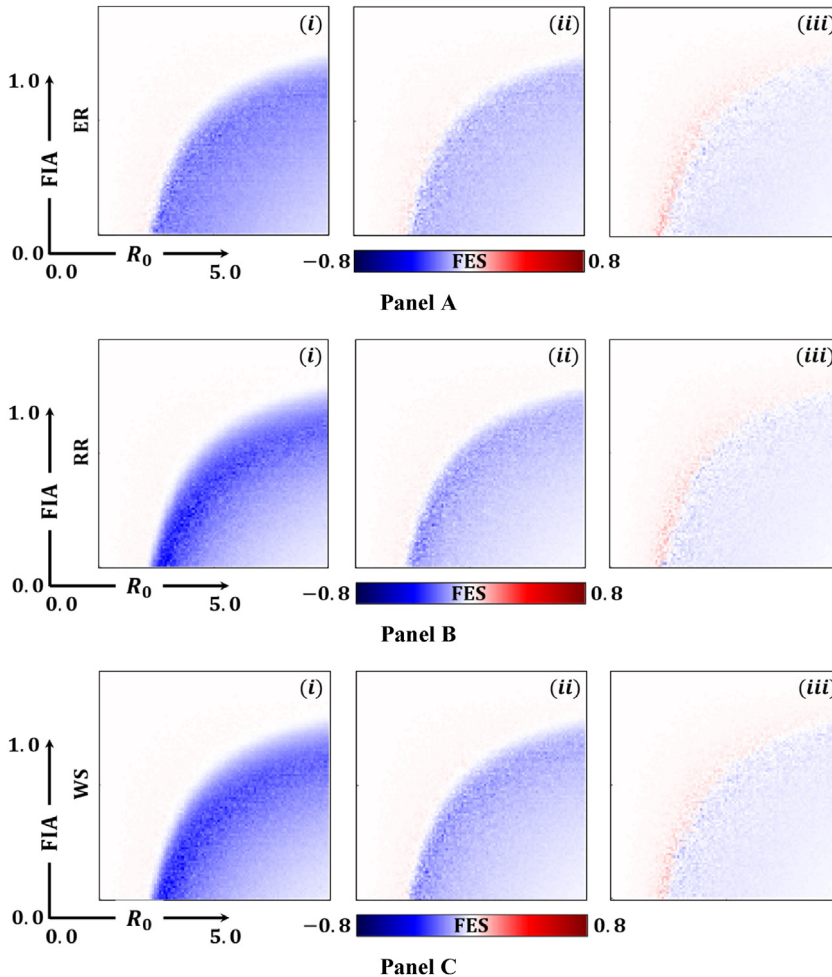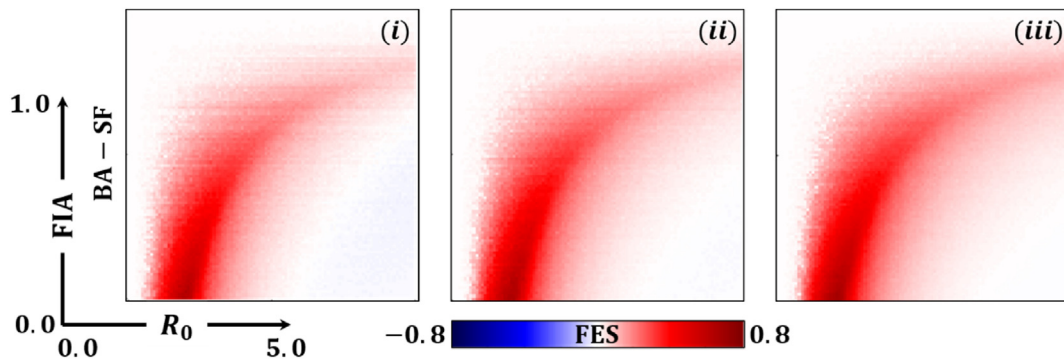

Figure: 5. Presented disease severity through 2D heat maps of the final epidemic size (FES) of the individuals concerning the basic reproduction number (R_0) and the fraction of immunized agents (FIA) in ER random, RR, and WS networks. Subpanels A, B, and C show for ER random, RR, and WS physical networks. Here, we subtract deterministic results from the degree (i) $<k> = 8,$ (ii) $<k> = 16,$ and (iii) $<k> = 64$. The total population $N = 10^4, \gamma = \frac{1}{3}$.
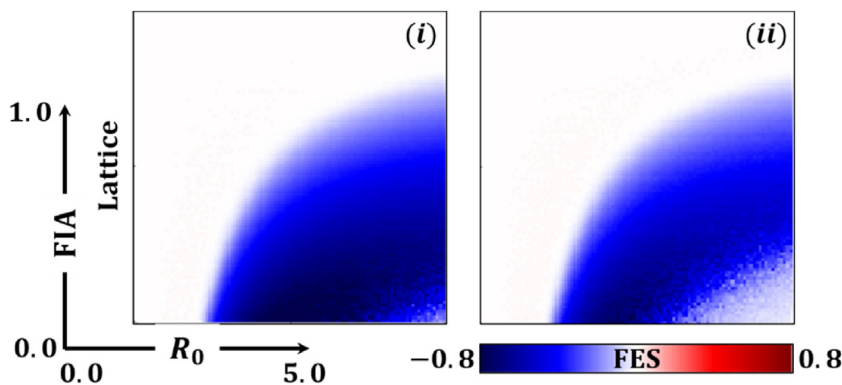
Figure: 6. Presented disease severity through 2D heat maps of the final epidemic size (FES) of the individuals concerning the basic reproduction number (R_0) and the fraction of immunized agents (*FIA*) in BA-SF networks. Here, we subtract deterministic results from the degree (i) $<k> = 8$, (ii) $<k> = 16$, and (iii) $<k> = 64$. The total population $N = 10^4, \gamma = \frac{1}{3}$.
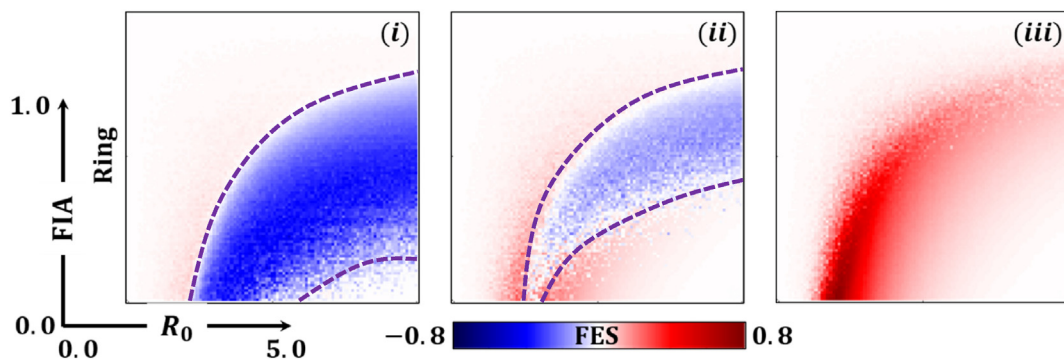

Figure: 7. Presented disease severity through 2D heat maps of the final epidemic size (FES) of the individuals concerning the basic reproduction number (R_0) and the fraction of immunized agents (*FIA*) in Lattice networks. Here, we subtract deterministic results from the degree (i) $<k> = 4$ and (iii) $<k> = 8$. The total population $N = 10^4, \gamma = \frac{1}{3}$.

Figure: 8. Presented disease severity through 2D heat maps of the final epidemic size (FES) of the individuals concerning the basic reproduction number (R_0) and the fraction of immunized agents (*FIA*) in Ring networks. Here, we subtract deterministic results from the degree (i) $<k> = 8$, (ii) $<k> = 16$, and (iii) $<k> = 64$. The total population $N = 10^4, \gamma = \frac{1}{3}$.

have a low degree; the disease can spread more quickly because the highly connected nodes can act as hubs for the infection to spread to many other nodes.

Furthermore, the BA network is particularly vulnerable to targeted attacks, where the most interconnected nodes are removed; removing hubs can quickly fragment the network into smaller, separate components, limiting the spread of the
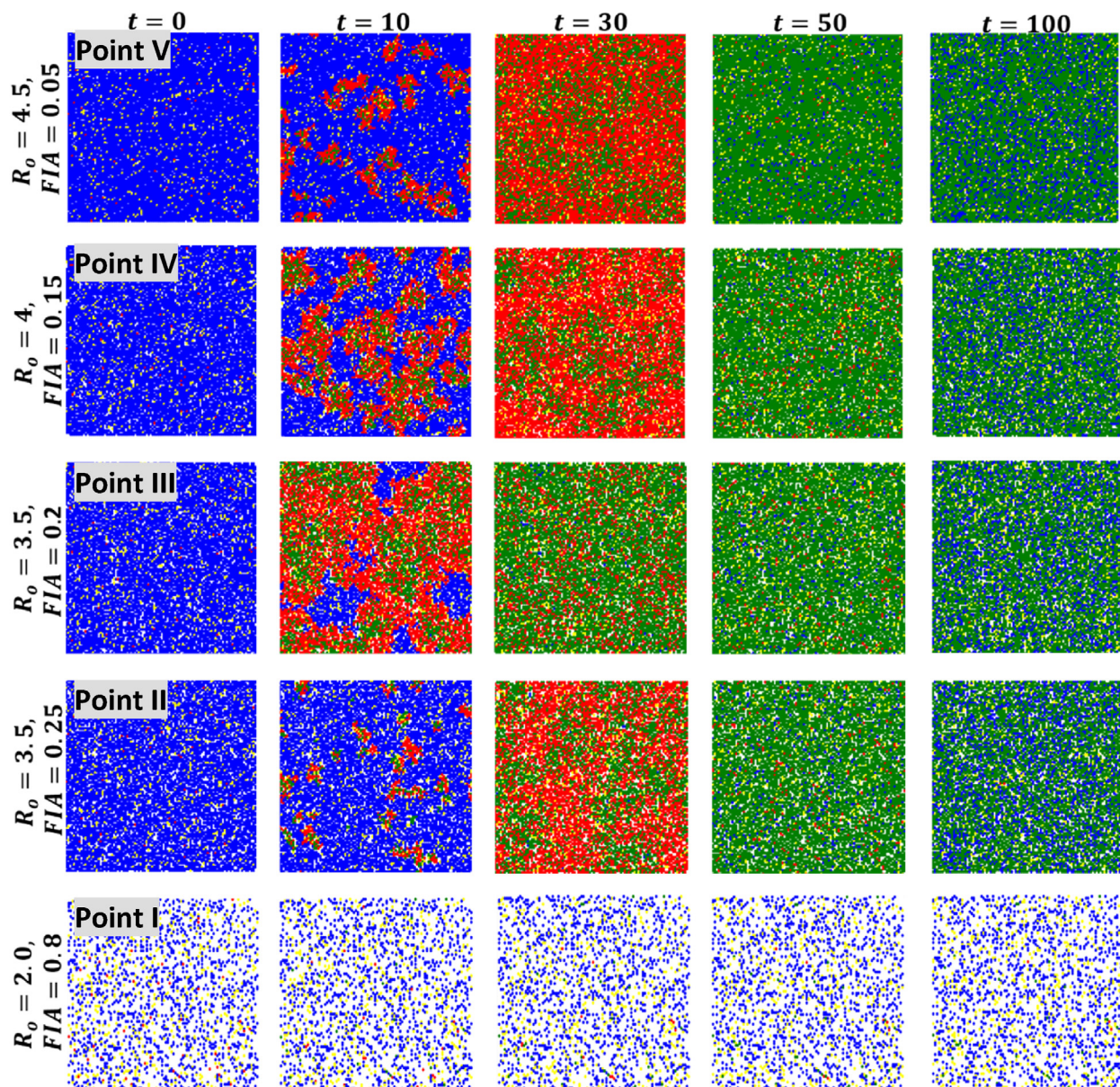
Figure: 9. The subsystem presents a spreading graph by considering both birthrate and death rate of five points taken from block f(ii) in Fig. 4 (Panel A) for the Lattice structure with $<k> = 8$. This figure is a counter graph of Fig. 4 (Panel B). The points are ((R_0, FIA)= (2.0, 0.8), (3.5, 0.25), (3.5, 0.2), (4.0, 0.15), and (4.5, 0.05). The blue, red, green, yellow and white colors display number of susceptible, infected, recovered, Empty, and void (immunized) individuals, respectively. Here, $Empty = 0.05, \Lambda = 0.01$, and $\mu = 0.01$. The leftmost panel shows the initial setup at $t = 0$. Other columns are presented for time step $t = 10, t = 30, t = 50$, and $t = 100$.

disease. Random networks or regular lattices may be more resilient to targeted attacks than other networks, as they lack hubs critical to the network's connectivity. Finally, the BA network's scale-free structure can significantly affect epidemic spread and control, making it an essential model for understanding disease dynamics in real-world networks.

Lattice is a type of network with a highly organized structure where it is not feasible to disrupt the pattern, and the locations of the agents remain fixed permanently (Fig. 7). Such network structures can be compared with a structured population, which is not a well-mixed situation and is usually for a particular community, not the general public. Thus, the Lattice network structure mechanism is the best strategy to combat epidemics and pandemics because of its low disease severity (blue region).
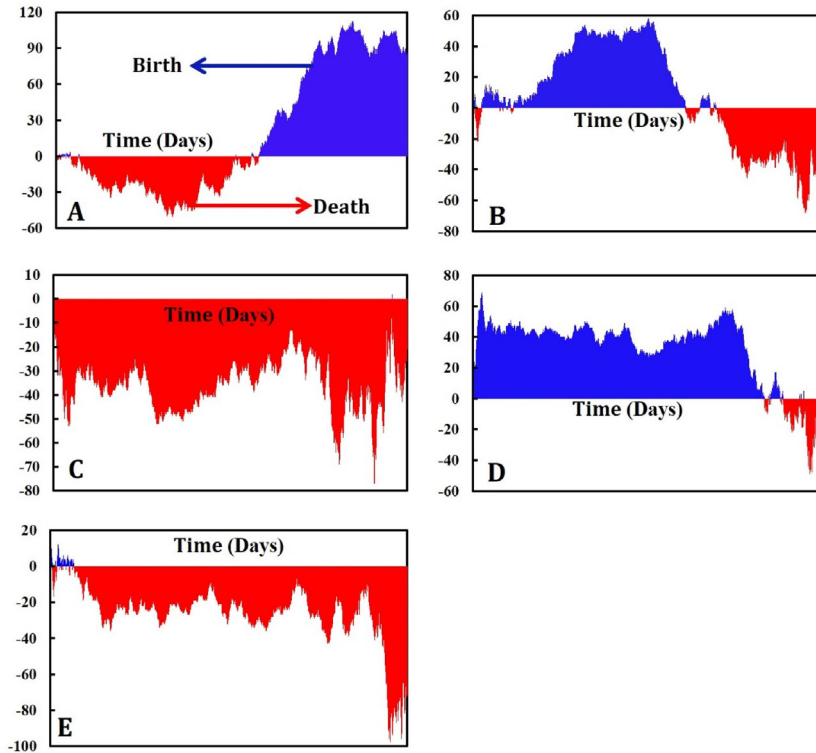
Figure: 10. The subsystem displays the entry and exit of birth and death agents from an empty node over elapsed time for a lattice structure with an average degree $<k> = 8$. This is illustrated in Fig. 9 (Panel A) for birth and death agents. The specified points are $(R_0, FIA) =$ (A) (2.0, 0.8), (B) (3.5, 0.25), (C) (3.5, 0.2), (D) (4.0, 0.15), and (E) (4.5, 0.05). In the figure, blue represents the number of new births, while red indicates the number of deaths. Parameters are set as follows: $Empty = 0.05$, $\Lambda = 0.01$, and $\mu = 0.01$.

Finally, Fig. 8 illustrates the disease severity situation of Ring networks, where both red and blue regions are observed for $<k> = 8$, and the entirely red (higher severity) region is seen for $<k> = 64$. Here, increasing the degree of a ring network can increase the spread of disease because higher degrees correspond to more connections between nodes, meaning that individuals in the network have more direct contact with others, increasing the likelihood of disease transmission from one individual to another. Additionally, as the degree of the network increases, there may be more shortcuts between distant nodes, which can allow the disease transmission mechanism to move more quickly throughout the complex network. Therefore, a higher degree of connectivity in a ring network can lead to a faster and more extensive spread of disease.

We now incorporate the concept of birth and death agents into our epidemic model by considering the role of the Empty node. Some agents will be born from an empty node and contribute as susceptible agents. Conversely, some agents will die and remain in the Empty node. Using this concept of the Empty node for birth and death agents, we draw Figs. 9 and 10.

In Fig. 9, we present a spreading graph that accounts for both the birth and death rates at five points taken from block f(ii) in Fig. 4 (Panel A) for the lattice structure with an average degree $<k> = 8$. This figure serves as a counterpart to Fig. 4 (Panel B). The points are $(R_0, FIA) =$ (2.0, 0.8), (3.5, 0.25), (3.5, 0.2), (4.0, 0.15), and (4.5, 0.05). In the figure, blue, red, green, yellow, and white represent the number of susceptible, infected, recovered, Empty, and void (immunized) individuals, respectively. Parameters are set as follows: $Empty = 0.05$, $\Lambda = 0.01$, and $\mu = 0.01$. The leftmost panel shows the initial setup at $t = 0$. Other columns present snapshots at time steps $t = 10, t = 30, t = 50$, and $t = 100$.

In the context of epidemic diseases, it has been observed that when a significant proportion of the population, around 80%, has been immunized against existing diseases, the spread of the disease is effectively halted. However, it is essential to note that there may still be a small proportion of individuals who are not immune despite the high FIA rate. These individuals may still be susceptible to the disease and can transmit it to others, potentially leading to localized outbreaks or clusters of infections. The likelihood of such outbreaks occurring is influenced by the factors of birth and death agents on Empty nodes. Thus, it can be observed that introducing the concept of birth and death rates as Empty nodes has a significant impact on epidemic dynamics.

In Fig. 10, we display the entry and exit of birth and death agents from an empty node over elapsed time for a lattice structure with an average degree $<k> = 8$. In this figure, blue represents the number of new births, while red indicates the number of deaths. By considering the inclusion of birth and death agents through the Empty node concept, we gain a more comprehensive understanding of the dynamic interactions within the population during an epidemic. This approach highlights the importance of accounting for population changes due to births and deaths in modeling the spread of infectious diseases and their containment strategies.

3. Conclusion

This research systematically analyses the network's (ER Random, RR, BA-SF, Ring, Lattice, and WS) topology, average degree distribution, and several infection states to reveal the gap between structural population on disease incidence and severity. The concept of immunized nodes or agents (individuals) defined as void effects is also incorporated to provide an in-depth summary of the uses of a physical network in epidemiology. More precisely, the FIA of void nodes directly affects the FES when void nodes are randomly dispersed in the networks, i.e., void nodes act as barriers or buffers between infected individuals, limiting the disease's ability to propagate via the network. We have outlined the many diverse contributions to our knowledge of the processes behind spreading infectious diseases, focusing on those that entail physical contact. From among the systems that include physical interactions, we have separated network models and multi-agent-based models. In varied degrees, these models mimic the intricacy of physical networks, but they still fall short of solutions that include real interactions. In particular, we have shown that graph labeling and link mining can be pretty helpful for the current approaches. Incorporating birth and death agents into the epidemic model via Empty nodes significantly impacts epidemic dynamics. This approach emphasizes the importance of population dynamics in modeling infectious disease spread and containment strategies. It reveals that high immunization rates can effectively halt disease transmission despite the presence of susceptible individuals. We have explained the precise conditions under which these techniques show promise when used with a network model. We thus want to implement these concepts as soon as possible and compare them to rival techniques based simply on different centrality assessments. In the long term, it is fascinating to leverage the modeling power of multi-agent systems to get richer data from simulations for supply to analytical tools, which may be done by employing the modeling capabilities of multi-agent systems.

Data availability statement

The data supporting this study's findings are available from the corresponding author upon reasonable request.

Funding

CRediT authorship contribution statement

M.D. Shahidul Islam: Writing – original draft, Visualization, Software, Methodology, Data curation. **Mohammad Sharif Ullah:** Writing – original draft, Visualization, Validation, Methodology, Investigation, Formal analysis. **K.M. Ariful Kabir:** Writing – review & editing, Validation, Supervision, Investigation, Formal analysis, Conceptualization.

Declaration of competing interest

The authors declare that they have no known competing financial interests or personal relationships that could have appeared to influence the work reported in this paper.
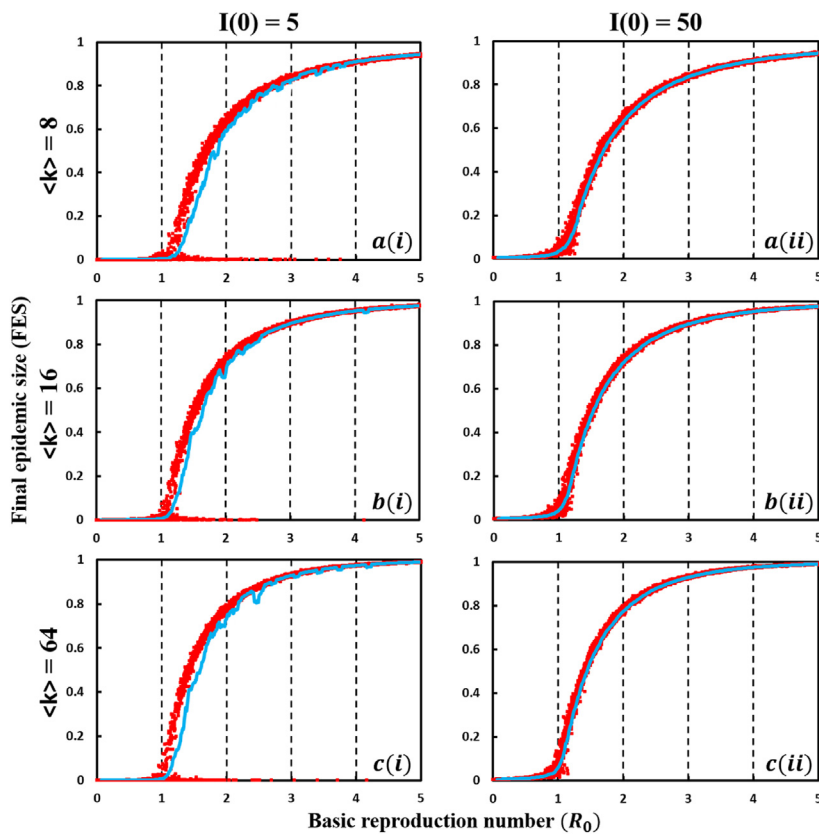
Appendix

Figure-A1. Representations of the basic reproduction number (R_0) versus the final epidemic size (FES) of ER random physical networks for initially infected individuals, (*-i) $I(0) = 5$ and (*-ii) $I(0) = 50$ with varying degrees of connectivity. Blue represents the average FES. Subpanels (a*), (b*), and (c*) show ER random physical networks for the average degree $<k> = 8, 16, 64$. Here, total population $N = 10^4$, *ensembles number* $100, \gamma = \frac{1}{3}$.
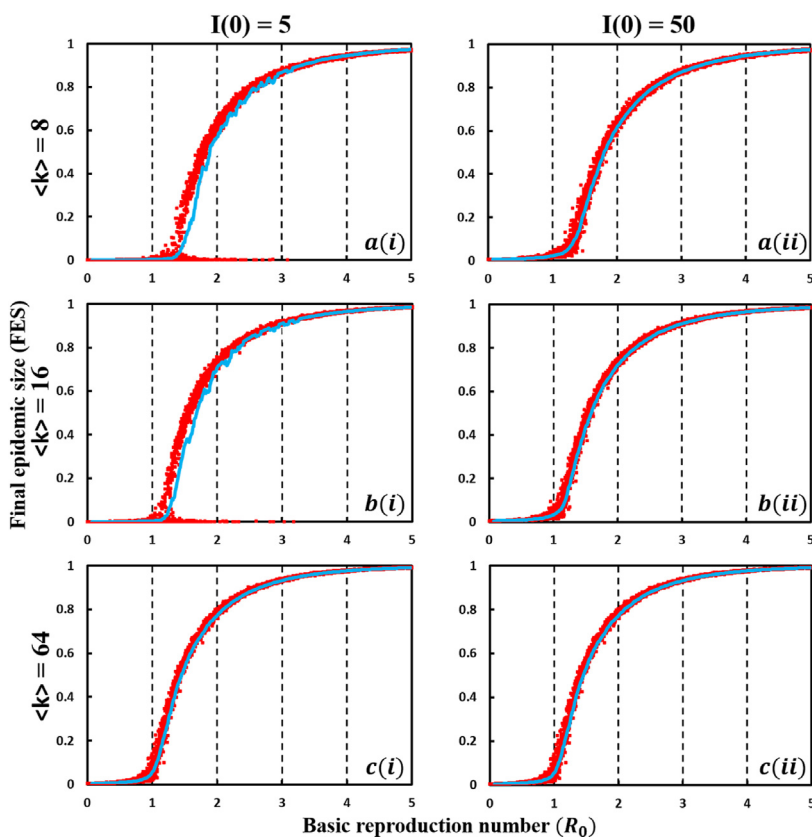
Figure-A2. Representations of the basic reproduction number (R_0) versus the final epidemic size (FES) of RR physical networks for initially infected individuals, (*-i) $I(0) = 5$ and (*-ii) $I(0) = 50$ with varying degrees of connectivity. Blue represents the average FES. Subpanels (a*), (b*), and (c*) show RR random physical networks for the average degree $<k> = 8, 16, 64$. Here, total population $N = 10^4$, *ensembles number* 100, $\gamma = \frac{1}{3}$.
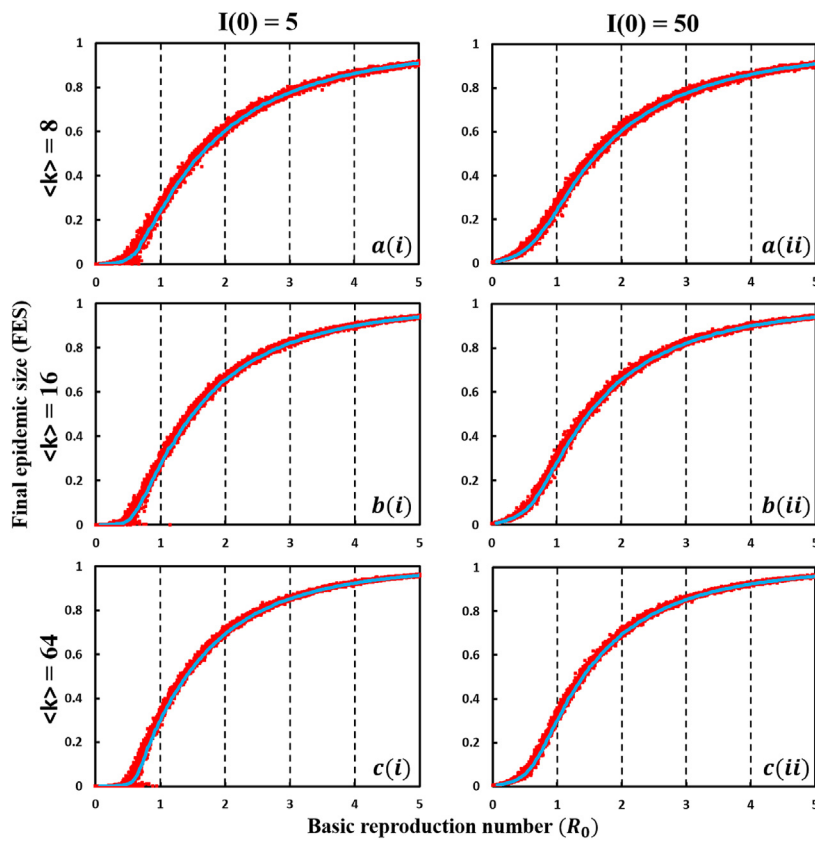
Figure-A3. Representations of the basic reproduction number (R_0) versus the final epidemic size (FES) of BA-SF physical networks for initially infected individuals, (*-i) $I(0) = 5$ and (*-ii) $I(0) = 50$ with varying degrees of connectivity. Blue represents the average FES. Subpanels (a*), (b*), and (c*) show BA-SF random physical networks for the average degree $<k> = 8, 16, 64$. Here, total population $N = 10^4$, $ensembles\ number\ 100, \gamma = \frac{1}{3}$.
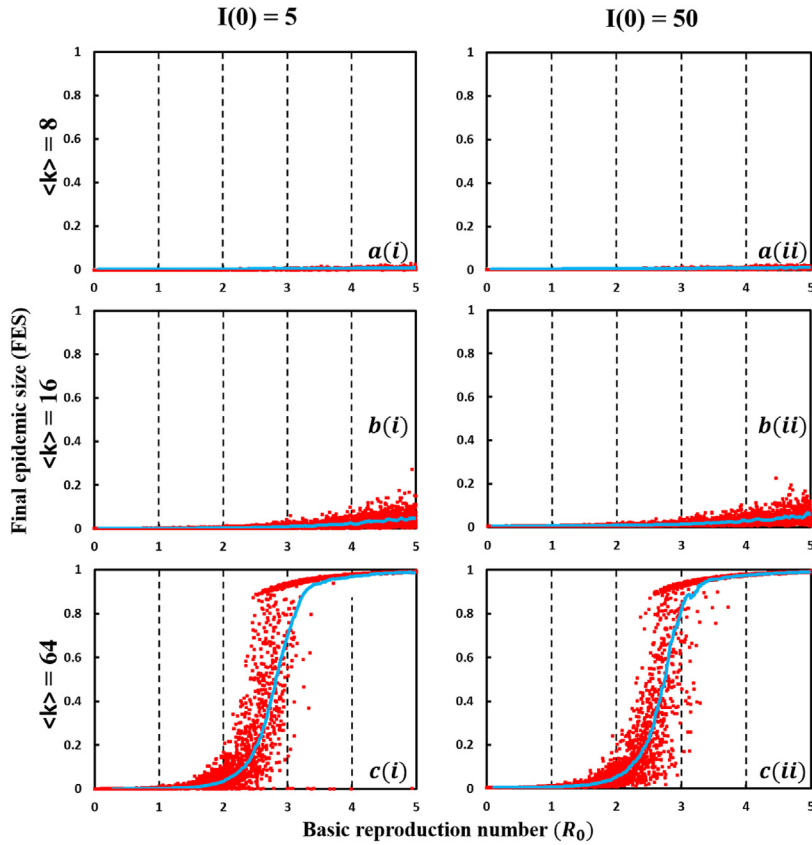
Figure-A4. Representations of the basic reproduction number (R_0) versus the final epidemic size (FES) of Ring physical networks for initially infected individuals, (*-i) $I(0) = 5$ and (*-ii) $I(0) = 50$ with varying degrees of connectivity. Blue represents the average FES. Subpanels (a*), (b*), and (c*) show Ring random physical networks for the average degree $<k> = 8, 16, 64$. Here, total population $N = 10^4$, *ensembles number* $100, \gamma = \frac{1}{3}$.

Figure-A5. Representations of the basic reproduction number (R_0) versus the final epidemic size (FES) of Lattice physical networks for initially infected individuals, (*-i) $I(0) = 5$ and (*-ii) $I(0) = 50$ with varying degrees of connectivity. Blue represents the average FES. Subpanels (a*), (b*), and (c*) show Lattice random physical networks for the average degree $<k> = 4, 8$. Here, total population $N = 10^4$, ensembles number $100, \gamma = \frac{1}{3}$.
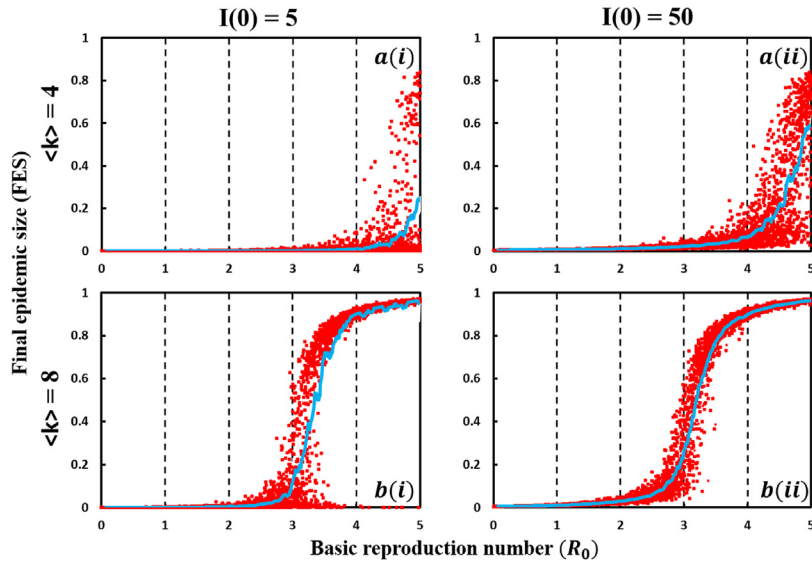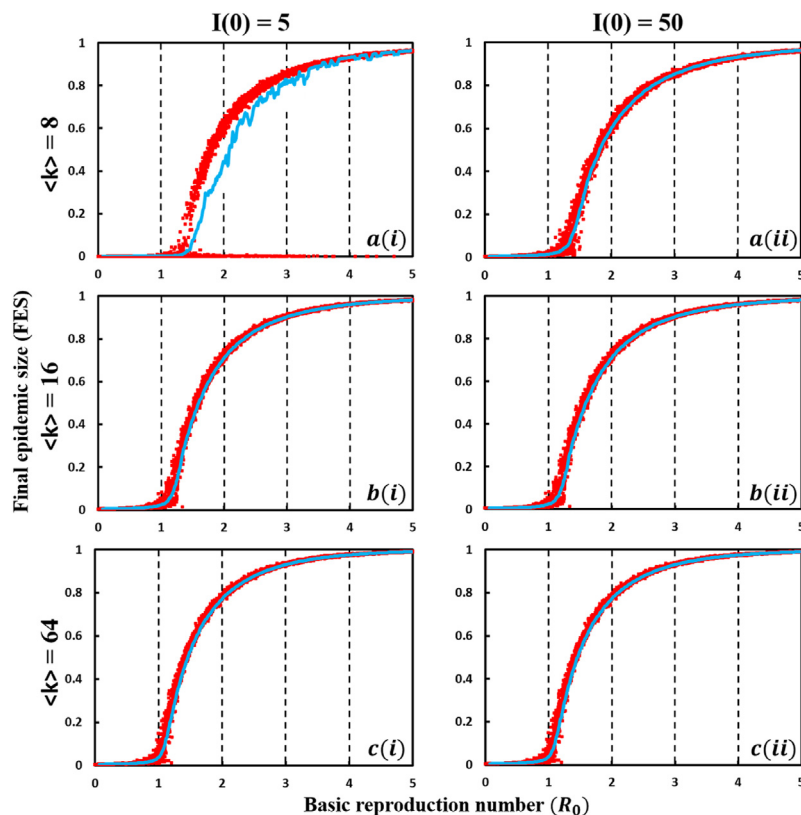
Figure-A6. Representations of the basic reproduction number (R_0) versus the final epidemic size (FES) of WS physical networks for initially infected individuals, (*-i) $I(0) = 5$ and (*-ii) $I(0) = 50$ with varying degrees of connectivity. Blue represents the average FES. Subpanels (a*), (b*), and (c*) show WS random physical networks for the average degree $<k> = 8, 16, 64$. Here, total population $N = 10^4$, *ensembles number* 100, $\gamma = \frac{1}{3}$.

References

Alexanderson, G. (2006). Euler and konigsberg's bridges: A historical view. *Bulletin of the American Mathematical Society, 43*, 567—571.

Allen, L. J. (2008). An introduction to stochastic epidemic models. *Mathematical Biosciences and Engineering, 5*(3), 435—446.

Atifa, A., Khan, M. A., Iskakova, K., Al-Duais, F. S., & Ahmad, I. (2022). Mathematical modeling and analysis of the SARS-Cov-2 disease with reinfection. *Computational Biology and Chemistry, 98*, Article 107678. https://doi.org/10.1016/j.compbiolchem.2022.107678

Barabási, A.-L. (2016). *Network science*. Cambridge, UK: Cambridge University Press.

Barabási, A. L., & Albert, R. (1999). Emergence of scaling in random networks. *Science, 286*(5439), 509—512.

Barnes, J. A. (1954). Class and committees in a Norwegian island parish. *Human Relations, 7*, 39—58.

Boguna, M., Pastor-Satorras, R., & Vespignani, A. (2003). Absence of epidemic threshold in scale-free networks with degree correlations. *Physical Review Letters, 90*, Article 028701.

Bollobás, B. (2001). *Random graphs* (Vol. 73). Cambridge University Press.

Caldarelli, G., & Catanzaro, M. (2012). *Networks: A very short introduction*. Oxford, U.K.: Oxford University Press.

Callaway, D. S., Newman, M., Strogatz, S. H., & Watts, D. J. (2000). Network robustness and fragility: Percolation on random graphs. *Physical Review Letters, 85*, 5468—5471.

Cayley, A. (1857). On the symmetric functions of the roots of certain systems of two equations. *Philosophical Transactions of the Royal Society of London*, (147), 717—726.

Chen, S., Small, M., Tao, Y., & Fu, X. (2018). Transmission dynamics of an SIS model with age structure on heterogeneous networks. *Bulletin of Mathematical Biology, 80*(8), 2049—2087. https://doi.org/10.1007/s11538-018-0445-z

Christakis, N. A., & Fowler, J. H. (2010). Social network sensors for early detection of contagious outbreaks. *PLoS One, 5*(9), 9.

Diekmann, O., Heesterbeek, J. A. P., & Metz, J. A. J. (1990). On the definition and the computation of the basic reproduction ratio R0 in models for infectious diseases in heterogeneous populations J. *Math. Biol., 28*, 365—382.

Driessche, V. P., & Watmough, J. (2002). Reproduction numbers and sub-threshold endemic equilibria for compartmental models of disease transmission Math. *BioScience, 180*, 29—48.

Erdős, P., & Rényi, A. (1959). On random graphs. *Publicationes Mathematicae, 6*(1), 290—297.

Erdös, P., & Rényi, A. (1960). On the evolution of random graphs. *Publ. Math. Inst. Hungar. Acad. Sci., 5*, 17—61.

Euler, L. (1741). Solutio problematis ad geometriam situs pertinentis. *Comment. Acad. Sci. Imp. Petropolitanae, 8*, 128—140.

Gillespie, D. T. (1977). Exact stochastic simulation of coupled chemical reactions. *Journal of Physical Chemistry, 81*(25), 2340—2361.

Goltsev, A. V., Dorogovtsev, S. N., Oliveira, J. G., & Mendes, J. F. F. (2012). Localization and spreading of diseases in complex networks. *Physical Review Letters, 109*, Article 128702.

Guo, H., Li, M. Y., & Shuai, Z. (2006). Global stability of the endemic equilibrium of multigroup SIR epidemic models. *Canadian Applied Mathematics Quarterly, 14*, 259—284.

Guo, H., Li, M. Y., & Shuai, Z. (2008). A graph-theoretic approach to the method of global Lyapunov functions. *Proceedings of the American Mathematical Society, 136*, 2793—2802.

Hamilton, W. R. (1858). Account of the icosian calculus. *Proc. R. Ir. Acad*, (6), 415—416.

Haq, I. U., Ullah, N., Ali, N., & Nisar, K. S. (2023). A new mathematical model of COVID-19 with quarantine and vaccination. *Mathematics, 11*(1), 142. https://doi.org/10.3390/math11010142

Kabir, K. M. A., Kuga, K., & Tanimoto, J. (2020). The impact of information spreading on epidemic vaccination game dynamics in a heterogeneous complex network- A theoretical approach. *Chaos, Solitons & Fractals, 132*, Article 109548.

Kabir, K. M. A., & Tanimoto, J. (2019a). Impact of awareness in metapopulation epidemic model to suppress the infected individuals for different graphs, European Physical. *Journal of Biology, 92*, 199.

Kabir, K. M. A., & Tanimoto, J. (2019b). Evolutionary vaccination game approach in metapopulation migration model with information spreading on different graphs. *Chaos, Solitons & Fractals, 120*, 41–55.

Kabir, K. M. A., & Tanimoto, M. S. (2023). Coupled simultaneous analysis of vaccine and self-awareness strategies on evolutionary dilemma aspect with various immunity. *Heliyon.* , Article e14355. https://doi.org/10.1016/j.heliyon.2023.e14355

Kirchhoff, G. (1845). On the motion of electricity in wires. *Philosophical Magazine A*, (13), 393–412.

Klovdahl, A. S. (1985). Social networks and the spread of infectious diseases: The aids example. *Social Science & Medicine, 21*(11), 1203–1216.

Kuga, K., & Tanimoto, J. (2022). Effects of void nodes on epidemic spreads in networks. *Scientific Reports, 12*, 3957. https://doi.org/10.1038/s41598-022-07985-9

LaSalle, J. P. (1977). The stability of dynamical systems. In *SIAM regional conference series in applied mathematics. No. 25*. Philadelphia: society for industrial and applied mathematics.

Li, M. Y., & Shuai, Z. (2010). Global-stability problem for coupled systems of differential equations on networks. *Journal of Differential Equations, 248*, 1–20.

Li, C. H., & Yousef, A. M. (2019). Bifurcation analysis of a network-based SIR epidemic model with saturated treatment function. *Chaos, 29*(3), Article 033129. https://doi.org/10.1063/1.5079631

Liljeros, F., Edling, C. R., Amaral, A. A. N., Stanley, H.e., & Aberg, Y. (2001). The web of human sexual contacts. *Nature, 411*, 907–908.

Lou, J., & Ruggeri, T. (2010). The dynamics of spreading and immune strategies of sexually transmitted diseases on scale-free network. *Journal of Mathematical Analysis and Applications, 365*(1), 210–219. https://doi.org/10.1016/j.jmaa.2009.10.044

Martcheva, M. (2015). *An introduction to mathematical epidemiology* (Vol. 61). New York: Springer.

Meyer, J. R., & Shackelton, L. A. (2019). Estimating the dynamics of endemic infections using stochastic models: A user's guide. *Biological Reviews, 94*(2), 502–520.

Milgram, S. (1967). The small world problem. *Psychology Today, 1*, 61–67.

Moreno, J. L. (1934). *Who shall survive? A new approach to the problem of human interrelations*. New York, NY, USA: Beacon House.

Moreno, Y., Pastor-Satorras, R., & Vespignani, A. (2002). Epidemic outbreaks in complex heterogeneous networks. *The European Physical Journal B, 26*, 521–529.

Newman, M. (2003). The structure and function of complex networks. *SIAM Review, 45*, 167–256.

Newman, M. (2018). *Networks* (2nd ed.). Oxford, UK: Oxford University Press.

Newman, M. E. J., Barabási, A. L., & Watts, D. J. (2006). *The structure and dynamics of networks*. Princeton University Press.

Ngonghala, C. N., Taboe, H. B., Safdar, S., & Gumel, A. B. (2023). Unraveling the dynamics of the Omicron and Delta variants of the 2019 coronavirus in the presence of vaccination, mask usage, and antiviral treatment. *Applied Mathematical Modelling, 114*, 447–465. https://doi.org/10.1016/j.apm.2022.09.017

Pastor-Satorras, R., & Vespignani, A. (2001). Epidemic spreading in scale-free networks. *Physical Review Letters, 86*, 3200–3203.

Pastor-Satorras, R., & Vespignani, A. (2002a). Epidemic dynamics in finite size scale-free networks. *Physical Review E - Statistical Physics, Plasmas, Fluids, and Related Interdisciplinary Topics, 65*, Article 035108.

Pastor-Satorras, R., & Vespignani, A. (2002b). Immunization of complex networks. *Physical Review E - Statistical Physics, Plasmas, Fluids, and Related Interdisciplinary Topics, 65*, Article 036104.

Ruoyan, S. (2010). Global stability of the endemic equilibrium of multigroup SIR models with nonlinear incidence. *Computers & Mathematics with Applications, 60*, 2286–2291.

Tatsukawa, Y., Arefin, M. R., Utsumi, S., Kuga, K., & Tanimoto, J. (2022). Stochasticity of disease spreading derived from the microscopic simulation approach for various physical contact networks. *Applied Mathematics and Computation, 431*, Article 127328. https://doi.org/10.1016/j.amc.2022.127328

Travers, J., & Milgram, S. (1969). An experimental study of the small world problem. *Sociometry, 32*, 425–443.

Ullah, M. S., Higazy, M., & Kabir, K. M. A. (2022a). Modeling the epidemic control measures in overcoming COVID-19 outbreaks: A fractional-order derivative approach. *Chaos, Solitons & Fractals.* https://doi.org/10.1016/j.chaos.2021.111636

Ullah, M. S., Higazy, M., & Kabir, K. A. (2022b). Dynamic analysis of mean-field and fractional-order epidemic vaccination strategies by evolutionary game approach. *Chaos, Solitons & Fractals, 162*, Article 112431. https://doi.org/10.1016/j.chaos.2022.112431

Wang, Z., Bauch, C. T., Bhattacharyya, S., Donofrio, A., Manfredi, P., Perc, M., Perra, N., Salathe, M., & Zhao, D. W. (2016). Statistical physics of vaccination. *Physics Reports, 664*, 1–114.

Wang, H., Wang, J., Ding, L., & Wei, W. (2017). Knowledge transmission model with consideration of self-learning mechanism in complex networks. *Applied Mathematics and Computation, 304*, 83–92. https://doi.org/10.1016/j.amc.2017.01.020

Watts, D. J., & Strogatz, S. H. (1998a). Collective dynamics of 'small-world' networks. *Nature, 393*(6684), 440–442.

Watts, D. J., & Strogatz, S. H. (1998b). Collective dynamics of 'small-world' networks. *Nature (London), 393*, 440–442 [CrossRef] [PubMed].

Wei, X. (2024). Global analysis of a network-based SIR epidemic model with a saturated treatment function. *International Journal of Biomathematics, 17*(6). https://doi.org/10.1142/s1793524523501127

Yang, J., Kuniya, T., & Luo, X. (2019). Competitive exclusion in a multi-strain SIS epidemic model on complex networks. *DOAJ (DOAJ: Directory of Open Access Journals)*. https://doaj.org/article/2e488a1d9dfb4c67a77e4853313de11b

Yang, J., & Xu, F. (2018). Global stability of two SIS epidemic mean-field models on complex networks: Lyapunov functional approach. *Journal of the Franklin Institute, 355*(14), 6763–6779. https://doi.org/10.1016/j.jfranklin.2018.06.040

Yuan, X., Wang, F., Xue, Y., & Liu, M. (2018). Global stability of an SIR model with differential infectivity on complex networks. *Physica, 499*, 443–456. https://doi.org/10.1016/j.physa.2018.02.065

Yuan, X., Xue, Y., & Liu, M. (2013a). Analysis of an epidemic model with awareness programs by media on complex networks. *Chaos, Solitons & Fractals, 48*, 1–11.

Yuan, X., Xue, Y., & Liu, M. (2013b). Dynamic analysis of a sexually transmitted disease model on complex networks. *Chinese Physics B, 22*(3), Article 030207.

Zhang, H. F., & Fu, X. C. (2009). Spreading of epidemics on scale-free networks with nonlinear infectivity. *Nonlinear Anal, 70*(9), 3273–3278.

Zhang, J. P., & Jin, Z. (2011). The analysis of an epidemic model on networks. *Applied Mathematics and Computation, 217*, 7053–7064.

Zhang, J. C., & Sun, J. T. (2014). Stability analysis of an SIS epidemic model with feedback mechanism on networks. *Physica A, 394*, 24–32.

Zhu, L., & Wang, Y. (2017). Rumor spreading model with noise interference in complex social networks. *Physica A: Statistical Mechanics and its Applications, 469*, 750–760. https://doi.org/10.1016/j.physa.2016.11.119